

KAP is the neuronal organelle adaptor for Kinesin-2 KIF3AB and KIF3AC

Alex Garbouchian, Andrew C. Montgomery, Susan P. Gilbert¹, and Marvin Bentley¹*

Department of Biological Sciences and Center for Biotechnology and Interdisciplinary Studies, Rensselaer Polytechnic Institute, Troy, NY 12180

ABSTRACT Kinesin-driven organelle transport is crucial for neuron development and maintenance, yet the mechanisms by which kinesins specifically bind their organelle cargoes remain undefined. In contrast to other transport kinesins, the neuronal function and specific organelle adaptors of heterodimeric Kinesin-2 family members KIF3AB and KIF3AC remain unknown. We developed a novel microscopy-based assay to define protein–protein interactions in intact neurons. The experiments found that both KIF3AB and KIF3AC bind kinesin-associated protein (KAP). These interactions are mediated by the distal C-terminal tail regions and not the coiled-coil domain. We used live-cell imaging in cultured hippocampal neurons to define the localization and trafficking parameters of KIF3AB and KIF3AC organelle populations. We discovered that KIF3AB/KAP and KIF3AC/KAP bind the same organelle populations and defined their transport parameters in axons and dendrites. The results also show that ~12% of KIF3 organelles contain the RNA-binding protein adenomatous polyposis coli. These data point toward a model in which KIF3AB and KIF3AC use KAP as their neuronal organelle adaptor and that these kinesins mediate transport of a range of organelles.

Monitoring Editor

Avital Rodal
Brandeis University

Received: Aug 15, 2022

Revised: Sep 13, 2022

Accepted: Sep 28, 2022

INTRODUCTION

The Kinesin-2 family consists of heterodimeric and homodimeric processive motors that mediate microtubule plus end-directed transport (Kondo *et al.*, 1994; Yamazaki *et al.*, 1995; Muresan *et al.*, 1998; Yang and Goldstein, 1998; Scholey, 2013; Guzik-Lendrum *et al.*, 2015; Gilbert *et al.*, 2018). Mammals express three heterodimeric Kinesin-2 proteins: KIF3A, KIF3B, and KIF3C, that assemble into two dimers, KIF3AB or KIF3AC. KIF3AB is the primary anterograde motor in intraflagellar transport (IFT) (Scholey, 2013; Milic *et al.*, 2017; Prevo *et al.*, 2017; Funabashi *et al.*, 2018; Lewis *et al.*,

2018; Engelke *et al.*, 2019) and binds IFT particles through the adaptor kinesin-associated protein 3B (KAP) (Wedaman *et al.*, 1996; Yamazaki *et al.*, 1996; Brunnbauer *et al.*, 2010; Scholey, 2013; Carpenter *et al.*, 2015; Funabashi *et al.*, 2018).

Beyond the well-defined role of KIF3AB/KAP in IFT, little is known about its other transport functions. KIF3AB/KAP is proposed to mediate transport of spectrin/fodrin (Takeda *et al.*, 2000) and RNA particles containing adenomatous polyposis coli (APC) (Jimbo *et al.*, 2002; Ruane *et al.*, 2016). The latter function was recently supported by elegant *in vitro* experiments showing that KIF3AB/KAP and APC assemble into a transport-capable complex, although neuronal evidence of this interaction is still outstanding (Baumann *et al.*, 2020). Even less is known about KIF3AC. KIF3C is highly expressed in the CNS (Muresan *et al.*, 1998; Sardella *et al.*, 1998; Navone *et al.*, 2001) and cultured hippocampal neurons (Silverman *et al.*, 2010), but its neuronal function is unclear. To date, the only proposed KIF3AC cargo is fragile-X mental retardation protein (FMRP) (Davidovic *et al.*, 2007), and KIF3CC homodimers may mediate microtubule dynamics in response to axon injury (Gumy *et al.*, 2013). Recent studies made some progress toward characterizing KIF3AB and KIF3AC in neurons. Constitutively active motor domain heterodimers of KIF3AB and KIF3AC can move on both axonal and dendritic microtubules (Huang and Banker, 2012). However, motor domain activity does not necessarily reflect transport preferences of kinesins that are associated with their vesicle cargoes (Nabb *et al.*, 2020).

This article was published online ahead of print in MBoc in Press (<http://www.molbiolcell.org/cgi/doi/10.1091/mbc.E22-08-0336>).

Conflict of interest: The authors declare no competing interest.

Author contributions: A.G. and A.M. designed and performed experiments, analyzed data, and wrote the manuscript. S.P.G. and M.B. supervised the research, conceptualized the study, designed experiments, and wrote the manuscript.

*Address correspondence to: Marvin Bentley (bentlm3@rpi.edu).

Abbreviations used: APC, adenomatous polyposis coli; FMRP, fragile-X mental retardation protein; IFT, intraflagellar transport; KAP, kinesin-associated protein 3B; NgCAM, neuron-glia cell adhesion molecule.

© 2022 Garbouchian *et al.* This article is distributed by The American Society for Cell Biology under license from the author(s). Two months after publication it is available to the public under an Attribution–Noncommercial–Share Alike 4.0 International Creative Commons License (<http://creativecommons.org/licenses/by-nc-sa/4.0>).

“ASCB®,” “The American Society for Cell Biology®,” and “Molecular Biology of the Cell®” are registered trademarks of The American Society for Cell Biology.

Beyond these initial studies, little is known about the neuronal function of KIF3AB and KIF3AC, raising the following questions: do KIF3AB and KIF3AC participate in neuronal organelle transport, what is the adaptor for organelle–cargo linkage, and what other proteins or motors associate with the KIF3 organelles in hippocampal neurons?

To address these questions, we applied two primary strategies in cultured hippocampal neurons. First, we developed a fluorescence-based assay to probe for protein–protein interactions in intact neurons. We systematically characterized the binding interactions of KIF3AB and KIF3AC with KAP and found that both KIF3AB and KIF3AC bind KAP. Moreover, the KAP-binding site for both heterodimers is localized in their C-terminal disordered domains. Second, we expressed the fluorescent kinesin tail domain in cultured hippocampal neurons to analyze the localization and trafficking parameters of organelle-bound kinesins (Yang *et al.*, 2019; Montgomery *et al.*, 2022). With this approach, we found that KIF3AB, KIF3AC, and KAP bind the same neuronal organelles. These organelles undergo sporadic long-range transport. A fraction of these organelles colocalize with the RNA-binding protein APC, indicating that KIF3/KAP likely interacts with additional neuronal cargoes. Results show that KIF3AB/KAP and KIF3AC/KAP participate in neuronal transport outside of IFT and that KAP is an organelle adaptor for KIF3AB and KIF3AC.

RESULTS

A novel microscopy-based protein–protein interaction assay reveals that KAP binds KIF3AB and KIF3AC

KIF3AB interaction with KAP is well established in IFT (Yamazaki *et al.*, 1996; Brunnbauer *et al.*, 2010; Verhey *et al.*, 2011; Gilbert *et al.*, 2018). In contrast, the function of KIF3AB and KIF3AC outside IFT is not well understood, especially in neurons. One key unknown is whether KIF3AB and KAP assemble in neurons outside of IFT. A second unknown is whether KIF3AC binds KAP. To determine KIF3–KAP interactions, we developed a fluorescence-based protein–protein binding assay in intact neurons (Figure 1A). Biochemical binding assays have long been the standard in the cell biological toolkit for determining protein–protein interactions. While powerful, we sought to determine interactions in their natural milieu, the cytoplasm of cultured hippocampal neurons, a highly specialized cell type (Arendt *et al.*, 2016, 2019; Bentley and Banker, 2016; Yogev and Shen, 2017).

The assay was designed to use inducible colocalization as the readout for binding between two proteins, in this case KAP and the candidate KIF3s. It involves expression of proteins tagged with the FK506 binding protein (FKBP) and FKBP12-rapamycin binding (FRB) domains, which dimerize in the presence of a rapamycin analogue linker molecule (Belshaw *et al.*, 1996; Banaszynski *et al.*, 2005; Kapitein *et al.*, 2010; Robinson *et al.*, 2010; Jenkins *et al.*, 2012; Bentley and Banker, 2015; Bentley *et al.*, 2015) (Figure 1A). Candidate GFP-tagged kinesin tails and FRB-KAP were coexpressed with a construct consisting of an FKBP domain, a tdTomato fluorophore, and the peroxisomal protein Pex3 (PEX-tdTM-FKBP). Peroxisomes are convenient organelles because they are a distinct and largely stationary organelle population that is not thought to interact with KIF3s. Linker-specific colocalization of GFP-KIF3 and peroxisomes indicates specific interaction between FRB-KAP and the GFP-tagged candidate kinesin tail.

We first applied the assay to test for interactions between FRB-KAP and GFP-KIF3B³⁹¹⁻⁷⁴⁷ tail (Figure 1B), as there is a strong prediction for binding of these proteins. Both proteins were coexpressed with untagged KIF3A tail and PEX-tdTM-FKBP. High-magnification

images show that PEX-tdTM-FKBP was targeted to peroxisomes in dendrites, as anticipated (Kapitein *et al.*, 2010). GFP-KIF3B was mostly soluble in the absence of linker, and there was no colocalization with peroxisomes. In cells treated with 100 nM linker for 2 h, the distribution of peroxisomes was unchanged. In contrast, linker treatment resulted in GFP-KIF3B colocalization with peroxisomes. Not all GFP-KIF3B was targeted to peroxisomes; a soluble component remained in the cytoplasm. This is presumably because peroxisomal targeting is limited by the availability of FRB-KAP and PEX-tdTM-FKBP. However, any linker-specific colocalization is extraordinarily strong evidence that KIF3B and KAP specifically interact in neurons.

We next asked whether KIF3C tail (GFP-KIF3C⁴¹¹⁻⁷⁹⁶) binds KAP in neurons (Figure 1C). Without linker, GFP-KIF3C was mostly soluble and did not colocalize with peroxisomes. Treatment with linker targeted GFP-KIF3C to peroxisomes, indicating that KAP bound KIF3C. This is the first experimental evidence to show specific KAP–KIF3C interaction. This finding also suggests that KIF3/KAP interactions on organelles may differ from those on IFT, as KIF3C cannot replace KIF3B in IFT transport in cilia (Engelke *et al.*, 2019).

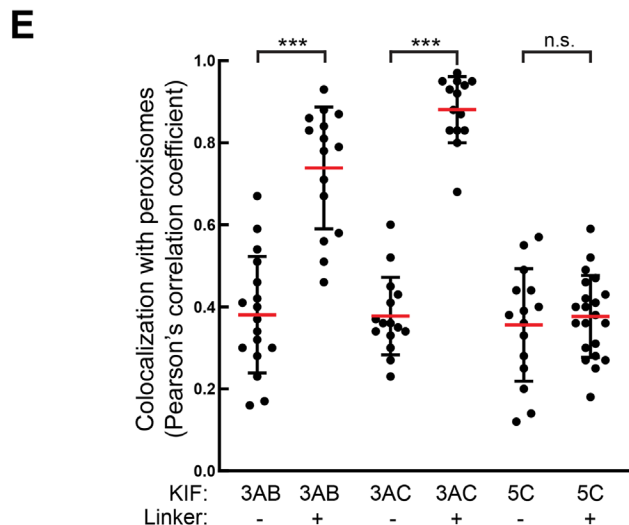
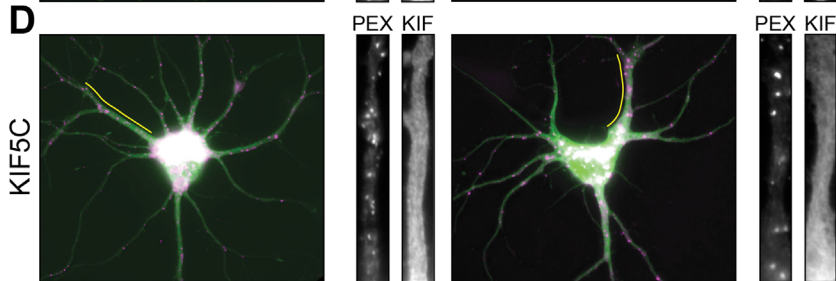
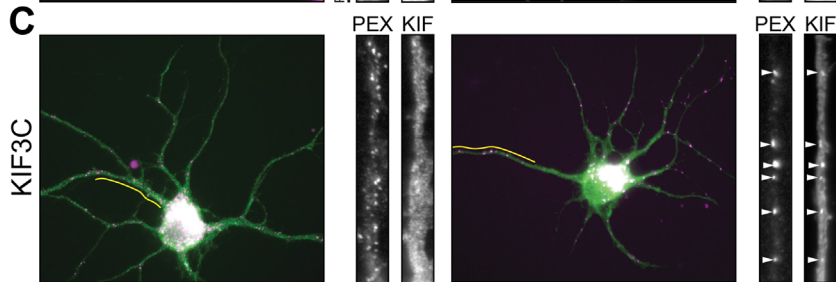
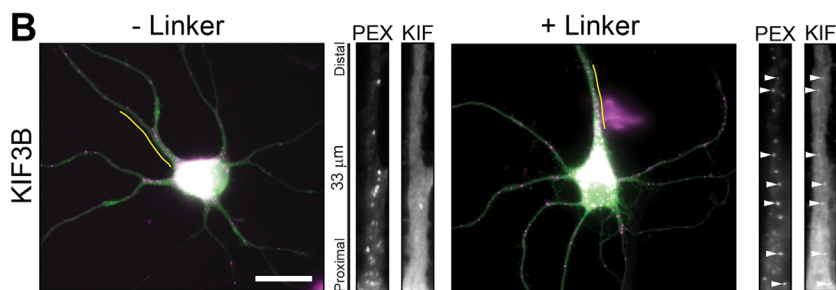
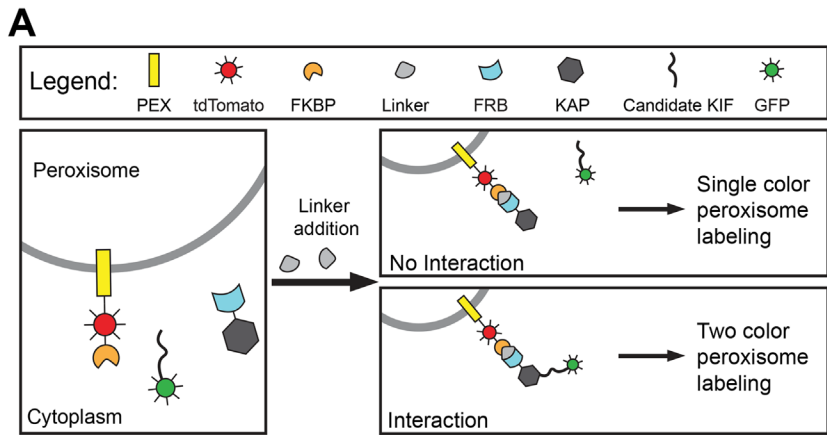
Finally, we tested GFP-KIF5C tail (GFP-KIF5C³⁷⁸⁻⁹⁵⁵) to confirm the specificity of the assay (Figure 1D). KIF5C is a member of the Kinesin-1 family that does not interact with KAP (Hackney *et al.*, 1991; Verhey *et al.*, 2001; Schnapp, 2003; Woźniak and Allan, 2006). As expected, linker treatment did not target GFP-KIF5C to peroxisomes, which confirms the specificity of the assay.

Because the readout of these experiments is colocalization of the candidate kinesin and peroxisomes, the Pearson's correlation coefficient is a convenient quantification method (Figure 1E). Without linker, correlation coefficients were consistently between 0.3 and 0.4, typical values for cellular structures and a largely soluble protein that does not specifically colocalize (Frank *et al.*, 2020). Linker addition and the resulting colocalization caused high coefficients for KIF3B (0.75) and KIF3C (0.88). The correlation coefficient for KIF5C was not changed by linker treatment. Together, these measurements show that KAP binds not just KIF3AB but also KIF3AC and that this assay is highly specific.

KIF3 tails dimerize without the N-terminal coiled-coil dimerization domain

The protein–protein binding assay allowed us to further investigate the KIF3AB/KAP and KIF3AC/KAP interactions. First, we asked whether KIF3 tails dimerize (Figure 2, A–D). These constructs lack the N-terminal motor, neck linker, and first coiled-coil domains that are sufficient for dimerization and generate constitutively active processive motors (Huang and Banker, 2012; Andreasson *et al.*, 2015; Guzik-Lendrum *et al.*, 2015; Phillips *et al.*, 2016; Guzik-Lendrum *et al.*, 2017; Gilbert *et al.*, 2018). GFP-KIF3B³⁹¹⁻⁷⁴⁷ (Figure 2C) or GFP-KIF3C⁴¹¹⁻⁷⁹⁶ (Figure 2D) was coexpressed with FRB-KIF3A and FKBP-tdTM-PEX. Linker treatment caused both GFP-tagged tails to colocalize with peroxisomes, which was accompanied by an increase in the Pearson's correlation coefficient (Figure 2E). These data show that KIF3AB and KIF3AC tails form dimers independent of the N-terminal motor and coiled-coil dimerization domains.

The fact that KIF3AB and KIF3AC tails form heterodimers may indicate that such dimerization is a prerequisite for binding KAP. Because kinesins are typically in a stable dimeric state, exogenously expressed tails are unlikely to dimerize with endogenous kinesins. Therefore, expressing one KIF3 tail without its dimerization partner will likely result in monomers that could not bind KAP if dimerization is a prerequisite for that interaction. To test this hypothesis, we expressed GFP-KIF3A, GFP-KIF3B, or GFP-KIF3C tail together with



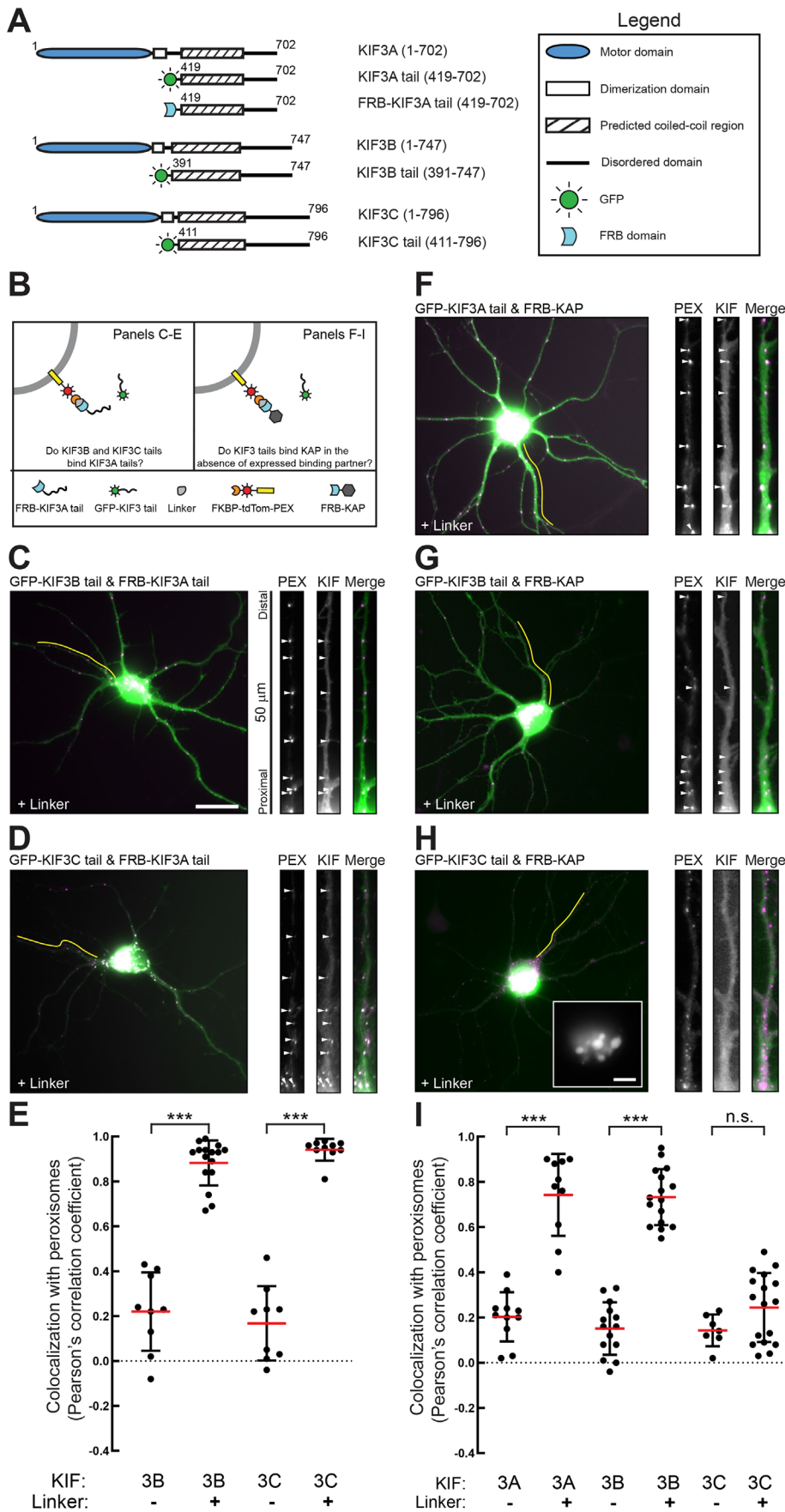
FRB-KAP and PEX-tdTM-FKBP. GFP-KIF3A (Figure 2F) and GFP-KIF3B (Figure 2G) both colocalized with peroxisomes after linker treatment, indicating that they can bind KAP as monomers. Quantification by Pearson correlation coefficient corroborated these results (Figure 2I). In contrast, GFP-KIF3C (Figure 2H) clustered in large protein aggregates in the soma instead of the mostly soluble distribution it exhibits when coexpressed with KIF3A (Figure 2D). Improperly folded proteins commonly form aggregates, and the fact that aggregates appeared only when GFP-KIF3C tail was expressed without KIF3A tail suggests that monomeric KIF3C does not fold properly. Therefore, KIF3CC homodimers are unlikely to form during normal development, although there may be exceptions to this in response to axon injury (Gumy *et al.*, 2013).

Disordered KIF3 C-terminal domains bind KAP

KIF3 tails are divided into two structural domains: a predicted coiled-coil domain and a C-terminal disordered domain (Yamazaki *et al.*, 1995; Wedaman *et al.*, 1996; Delorenzi and Speed, 2002; Gilbert *et al.*, 2018). Early electron microscopy studies proposed that KAP binds the C-terminal domain of KIF3AB (Wedaman *et al.*, 1996; Yamazaki *et al.*, 1996). In contrast, recent studies in *Drosophila* found that KAP binds the coiled-coil domain of heterodimeric KIF3 (Doodhi *et al.*, 2009; Ahmed *et al.*, 2020). Because KIF3AC-KAP interactions have not been reported before the present study, there are no proposed models for KIF3AC-KAP binding interactions.

To identify the KAP binding domains of KIF3A, KIF3B, and KIF3C, we generated fluorescently tagged expression constructs of the coiled-coil (KIF3^{CC}; Figure 3A) or disordered (KIF3^{DD}; Figure 4A) domains and determined whether each bound KAP. Because coexpression may be required for stable expression of KIF3, we first expressed each coiled-coil with its binding partner. We coexpressed GFP-KIF3A^{CC} and Halo-KIF3B^{CC} with FRB-KAP and PEX-tdTM-FKBP (Figure 3C). In a separate experiment, we coexpressed GFP-KIF3A^{CC} and Halo-KIF3C^{CC} with FRB-KAP and PEX-tdTM-FKBP (Figure 3D).

FIGURE 1: KIF3AB and KIF3AC both bind KAP. (A) Schematic illustrating the protein-protein interaction assay. Four proteins are expressed together: PEX-tdTM-FKBP, FRB-KAP, unlabeled KIF3A tail, and a GFP-tagged kinesin tail. Binding between KAP and the kinesin is evaluated by linker-induced colocalization of the GFP-tagged KIF3 tail with peroxisomes. (B–D) Representative images of 7 DIV hippocampal neurons expressing the indicated constructs. High-magnification images of dendrites were taken from the regions indicated by the yellow line. Arrowheads highlight examples of colocalization. Scale bar: 20 μm. (E) Quantification of colocalization between peroxisomes and kinesins. Cell sample sizes: KIF3AB(-): 15; KIF3AB(+): 15; KIF3AC(-): 15; KIF3AC(+): 14; KIF5C(-): 15; KIF5C(+): 21. ****p* < 0.001.



Halotags were visualized with JF646. Colocalization of each coiled-coil with peroxisomes was then quantified (Figure 3E). None of the coiled-coils was targeted to peroxisomes by linker addition, indicating that none of the coiled-coils interacted with KAP.

We next asked whether KIF3 coiled-coils behaved differently when expressed without their binding partner. Each coiled-coil (GFP-KIF3A^{CC}, GFP-KIF3B^{CC}, or GFP-KIF3C^{CC}) was coexpressed with FRB-KAP and PEX-tdTM-FKBP (Figure 3, F–H). All coiled-coil constructs expressed without forming aggregates. Linker treatment did not result in colocalization of coiled-coil domains with peroxisomes. Corresponding Pearson's correlation coefficients confirmed that linker treatment did not cause colocalization with peroxisomes (Figure 3I). Together, these results are strong evidence that mammalian KIF3 coiled-coils do not interact with KAP.

The finding that the coiled-coil domains of mammalian KIF3s do not interact with KAP predicts that the disordered C-terminal domain mediates interaction with KAP. We used the same systematic strategy to determine whether the disordered KIF3 domains bind KAP (Figure 4, A and B). We coexpressed GFP-KIF3A^{DD} and Halo-KIF3B^{DD} with FRB-KAP and PEX-tdTM-FKBP (Figure 4C). Next, we coexpressed GFP-KIF3A^{DD} and Halo-KIF3C^{DD} with FRB-KAP and PEX-tdTM-FKBP (Figure 4D). Colocalization of each KIF3 disordered domain with peroxisomes was quantified by Pearson's correlation coefficient (Figure 4E). All three KIF3

FIGURE 2: KIF3AB and KIF3AC dimerization does not require the canonical N-terminal dimerization domain. (A) Schematic illustrating the construct design. (B) Schematic illustrating the specific application of the protein-protein binding assay. (C, D, F–H) Representative images of 9 DIV neurons expressing the indicated proteins and treated with linker. High-magnification images of dendrites were taken from the regions indicated by the yellow line. Arrowheads highlight examples of colocalization. The inset in H shows GFP-KIF3C aggregates in the soma. Low-magnification scale bar: 20 μ m. High-magnification inset scale bar: 5 μ m. (E, I) Quantification of colocalization between peroxisomes and kinesins. Cell sample sizes, panel E: KIF3B(-): 10; KIF3B(+): 16; KIF3C(-): 9; KIF3C(+): 11. Cell sample size, panel I: KIF3A(-): 11; KIF3A(+): 10; KIF3B(-): 14; KIF3B(+): 16; KIF3C(-): 7; KIF3C(+): 17. *** $p < 0.001$.

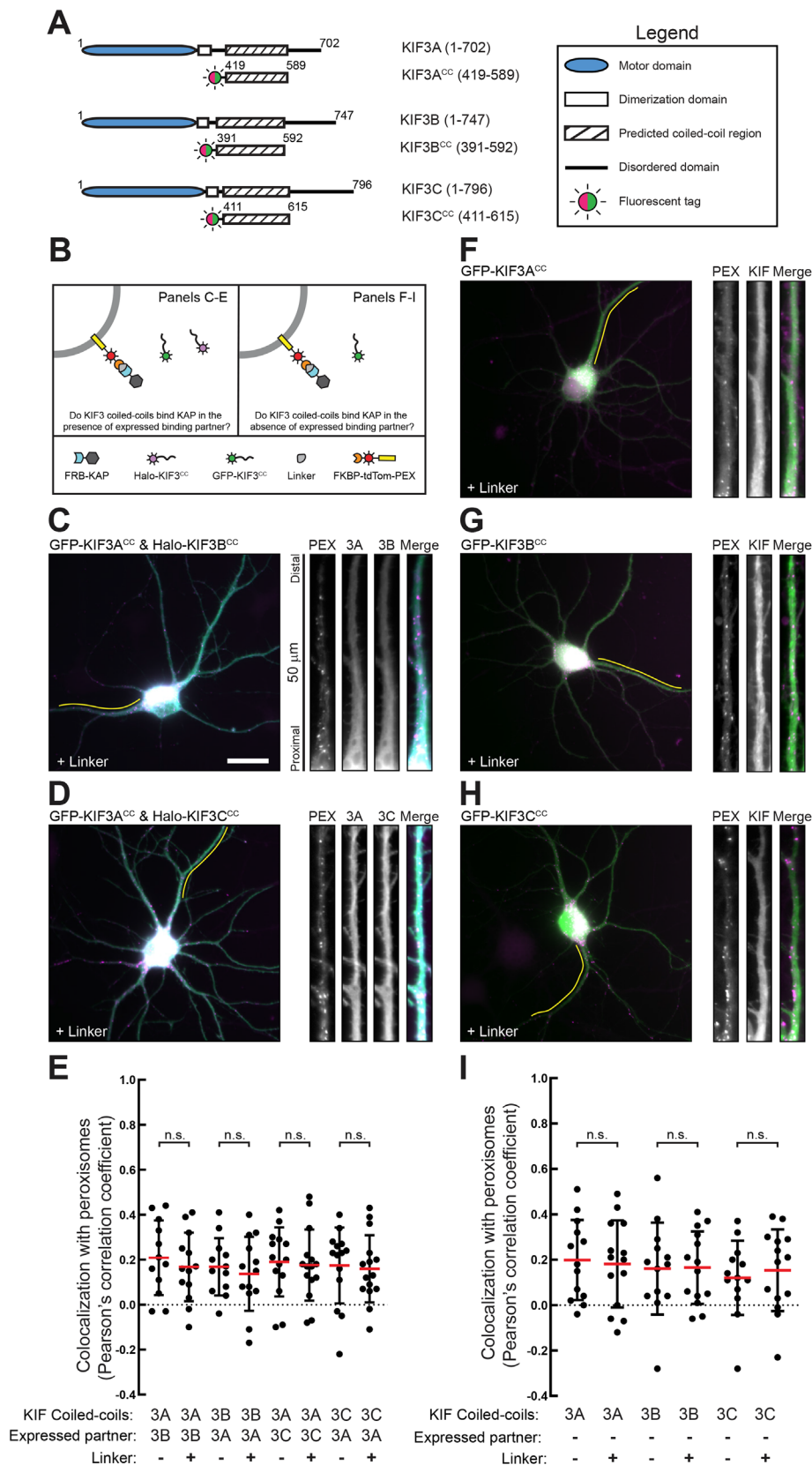


FIGURE 3: KAP binding to KIF3 is not mediated by coiled-coil domains. (A) Schematic showing the construct design. (B) Schematic illustrating the specific application of the protein-protein binding assay. (C, D, F–H) Representative images of 7 DIV neurons expressing the indicated proteins and treated with linker. High-magnification images of dendrites were taken from the regions indicated by the yellow line. Scale bar: 20 μ m. (E, I) Quantification of colocalization

disordered domains were targeted to peroxisomes in linker-treated neurons, showing that these domains alone are sufficient for binding KAP. A limitation of this experiment is that it cannot determine whether individual KIF3^{DD} bind to KAP, or whether KIF3A^{DD} and KIF3A^{CC} bind KAP as dimers. To address this, we coexpressed each disordered domain with FRB-KAP and PEX-tM-FKBP (Figure 4, F–H). Colocalization of KIF3 disordered domains with peroxisomes was quantified as before (Figure 4I). We first noticed that GFP-KIF3A^{DD} was not expressed properly. Instead of the expected soluble distribution, GFP-KIF3A^{DD} formed aggregates in the somatodendritic region. Aggregate formation was independent of linker incubation, and aggregates did not form when KIF3A^{DD} was coexpressed with either KIF3B^{DD} or KIF3C^{DD} (Figure 4, C–E). Therefore, the C-terminal disordered domains may dimerize independent of the coiled-coil domain. This is surprising, as coiled-coil domains are typically the primary sites of kinesin dimerization. In contrast, GFP-KIF3B^{DD} and GFP-KIF3C^{DD} were distributed through the cytoplasm without linker, and without any aggregate formation. Both colocalized with peroxisomes after linker treatment. This shows that KIF3B^{DD} and KIF3C^{DD} bind KAP and that this binding interaction does not depend on dimerization.

KIF3AB, KIF3AC, and KAP organelles exhibit similar cellular distributions and neuronal transport parameters

Because KIF3B and KIF3C both bind KAP, they may interact with some of the same neuronal organelle populations. We recently developed techniques for visualizing organelle-bound kinesins in live cells (Yang *et al.*, 2019; Frank *et al.*, 2020; Montgomery *et al.*, 2022). Improved organelle labeling was achieved by expressing the GFP-tagged kinesin tail domains, which mediate organelle binding. Using this approach, we generated initial recordings of organelle-bound KIF3B and KIF3C in neurons (Yang *et al.*, 2019). However, the signal-to-noise ratio in these experiments was low and may have missed any subpopulation of organelles that bound

between peroxisomes and kinesins. Cell sample sizes, panel E: KIF3A^{CC}(-): 12; KIF3A^{CC}(+): 15; KIF3B^{CC}(-): 14; KIF3B^{CC}(+): 15. Cell sample sizes, panel I: KIF3A^{CC}(-): 13; KIF3A^{CC}(+): 14; KIF3B^{CC}(-): 13; KIF3B^{CC}(+): 14; KIF3C^{CC}(-): 13; KIF3C^{CC}(+): 14. n.s. not significant.

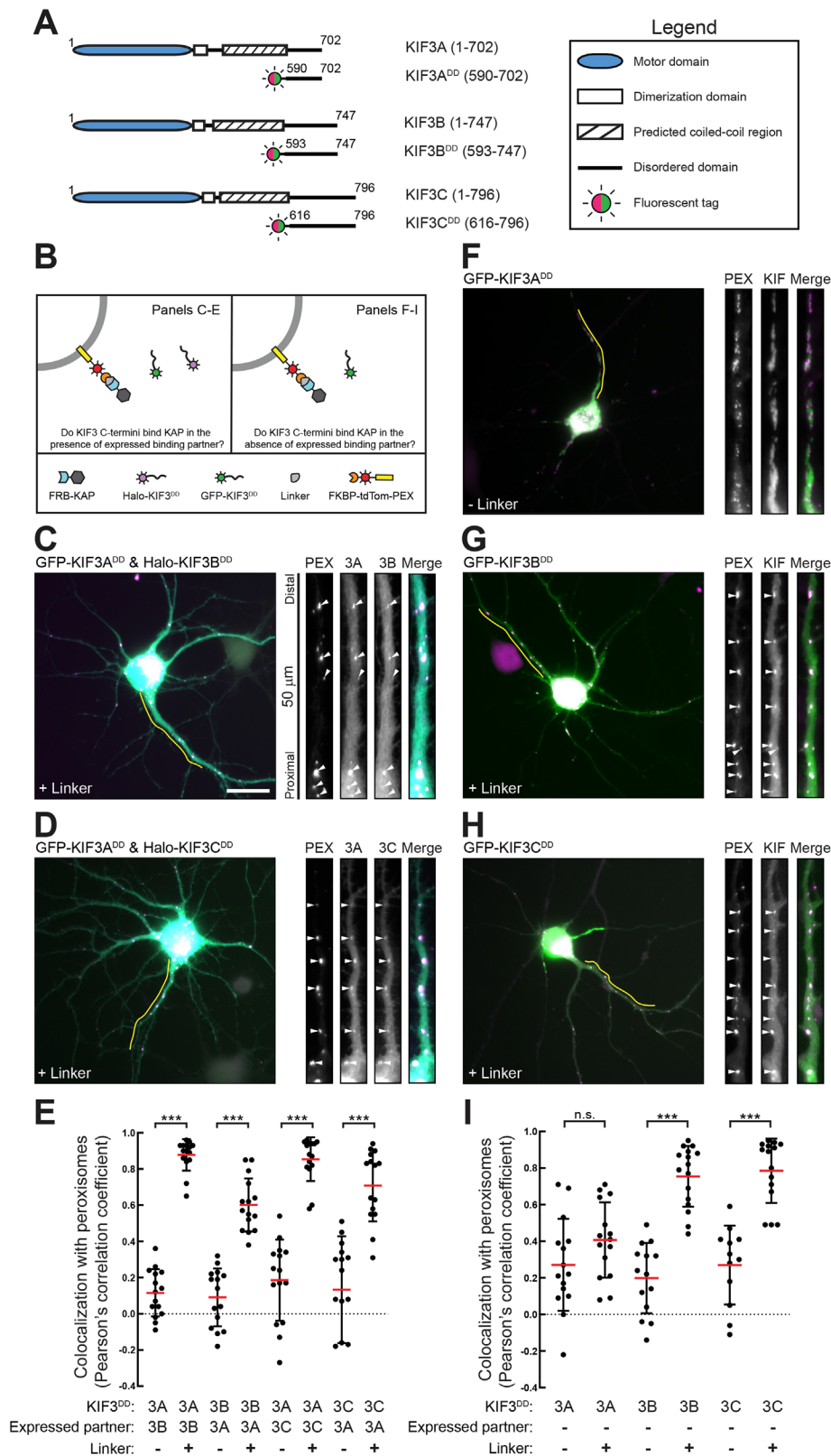


FIGURE 4: KAP binds the KIF3 C-terminal disordered domain. (A) Schematic showing the construct design. (B) Schematic illustrating the specific application of the protein-protein binding assay. (C, D, F–H) Representative images of 7 DIV neurons expressing the indicated proteins and treated with linker. High-magnification images of dendrites were taken from the regions indicated by the yellow line. Arrowheads highlight examples of colocalization. Scale bar: 20 μm . (E, I) Quantification of colocalization between peroxisomes and kinesins. Cell sample sizes, panel E: KIF3AB^{DD}(-): 15; KIF3AB^{DD}(+): 15; KIF3AC^{DD}(-): 15; KIF3AC^{DD}(+): 15. Cell sample

fewer kinesins, as they would be dim and challenging to image. It also prevented quantitative analysis of KIF3B and KIF3C organelle transport parameters.

To quantitatively assess the localization and transport parameters of KIF3AB and KIF3AC organelles, we sought to improve the technique. To facilitate recording at early expression times and improve visualization of dim organelles, we used the halotag system (Los *et al.*, 2008; Encell, 2012). The halotag enzyme itself is not fluorescent and becomes visible only after covalent binding to a fluorescent ligand. Bright organic dyes have substantially more favorable fluorescence characteristics than fluorescent proteins (Xia *et al.*, 2013; Grimm *et al.*, 2015) and enhance detection of organelle-bound proteins (Yang *et al.*, 2019; Frank *et al.*, 2020; Montgomery *et al.*, 2022). To use this approach, we generated halotagged KIF3B and KIF3C tail constructs (Figure 5A).

We expressed Halo-KIF3B (Figure 5B) or Halo-KIF3C (Figure 5C) tail in cultured hippocampal neurons and visualized halotag with JF549 (Grimm *et al.*, 2015). Because these kinesin tails form KIF3AB or KIF3AC dimers, we coexpressed nonfluorescent KIF3A tail to ensure that the dimerization partner was present at similar expression levels. This approach resulted in detectable organelles as early as 3 h after transfection.

Halo-KIF3B organelles were distributed throughout the neurons. High-magnification images from the axon and a dendrite show that organelles were consistently round and less than 1 μm in diameter. Corresponding kymographs show the movement of Halo-KIF3B organelles. On a kymograph, lines with a positive slope indicate anterograde movement and lines with a negative slope indicate retrograde movement. This convention is followed in all kymographs. Long-range transport events of Halo-KIF3B organelles were infrequent, and most did not extend beyond 5 μm .

Halo-KIF3C organelles exhibited a localization and morphology comparable to those of Halo-KIF3B (Figure 5C). Organelles were in both axon and dendrites, with infrequent long-range movements. One difference from KIF3B was that Halo-KIF3C tail expression consistently produced less cytoplasmic background than Halo-KIF3B. This higher signal-to-noise ratio eased detection

sizes, panel I: KIF3A^{DD}(-): 15; KIF3A^{DD}(+): 15; KIF3B^{DD}(-): 14; KIF3B^{DD}(+): 16; KIF3C^{DD}(-): 12; KIF3C^{DD}(+): 15. *** $p < 0.001$.

but did not result in a total increase in the number of labeled organelles.

Because both KIF3B and KIF3C bind KAP, these results suggest that KAP participates in the transport of neuronal KIF3AB and KIF3AC organelles. KAP is a globular protein with few known binding partners (Yamazaki *et al.*, 1996; Carpenter *et al.*, 2015), and little is known about its neuronal localization. We expressed Halo-KAP and visualized organelles with JF549 (Figure 5D). Halo-KAP labeled organelles in axons and dendrites. Most organelles had a round morphology, with a diameter $<1 \mu\text{m}$, comparable to that of KIF3B and KIF3C organelles. In the axon, KAP organelles underwent long-range transport with a strong anterograde bias. Halo-KAP expression resulted in very little cytoplasmic background fluorescence and consistent labeling.

Overall, KIF3B, KIF3C, and KAP organelles exhibited multiple commonalities. They were homogeneously distributed in axons and dendrites, exhibited comparable morphology, and underwent sporadic transport. Notably, despite differences in cytoplasmic background and the associated differences in the single-to-noise ratio, all three constructs labeled roughly the same number of organelles (see legend to Figure 5).

Achieving consistency in organelle labeling in combination with live-cell imaging allowed us to quantitatively assess the transport characteristics of each population. Each organelle in representative dendrite and axon segments was scored for its motility (Figure 5E). In the axon, most KIF3B, KIF3C, and KAP organelles were stationary. Retrograde movement was rare, exhibited by fewer than 7% of organelles. All three populations exhibited some amount of anterograde axonal movement. KAP exhibited the most active anterograde transport (25%), followed by KIF3B (12%) and KIF3C (10%). In dendrites the three populations behaved nearly identically. Movements were infrequent and without any directional bias. To evaluate directionality biases in transport, we determined the relative frequency of anterograde and retrograde movements in axons and dendrites by kymograph analysis (Figure 5, F and G). In axons, all three populations displayed an anterograde bias, although the bias was most pronounced for KAP. For all organelles, there were fewer overall transport events in dendrites. In dendrites, transport exhibited no directional bias, which is consistent with the fact that dendritic microtubules are less densely packed and have a mixed orientation (Baas *et al.*, 1988; Tas *et al.*, 2017).

Transport parameters differ between populations and act as a quantitative “signature” for specific organelles (Burack *et al.*, 2000; Niwa *et al.*, 2008; Lo *et al.*, 2011; Farfel-Becker *et al.*, 2019; van Bommel *et al.*, 2019; Yang *et al.*, 2019; Bodakuntla *et al.*, 2020; De Pace *et al.*, 2020; Frank *et al.*, 2020; Koppers and Farías, 2021). We systematically quantified the transport parameters (i.e., velocity and run length) of the three organelle populations (Figure 6). Histograms show run length and velocity measurements of KIF3B, KIF3C, and KAP moving anterograde or retrograde in axons or dendrites (Figure 6, A–D). KIF3B and KIF3C organelles behaved nearly identically. One difference between KIF3B and KIF3C organelles was in retrograde axonal movements, although this was likely due to variability caused by the relatively small number of total organelles undergoing retrograde movement in axons.

Mean organelle velocities, ranging from 0.31 to 0.49 $\mu\text{m/s}$, were slower than those of organelle populations that are moved by other kinesins (Takeda *et al.*, 2000; Niwa *et al.*, 2008; Yang *et al.*, 2019; Nabb and Bentley, 2022) but were comparable to the previously reported velocities for KIF3AB and KIF3AC in single-molecule motility experiments (Guzik-Lendrum *et al.*, 2015; Bensel *et al.*, 2017; Gilbert *et al.*, 2018; Woll *et al.*, 2018). KAP organelles consistently

exhibited velocities comparable to those of KIF3B and KIF3C. However, the mean anterograde run length of KAP organelles was 4.95 μm compared with 2.18 μm for KIF3B and 2.15 μm for KIF3C in axons.

There are at least three plausible explanations for this result. First, KAP may bind to some organelles without KIF3AB or KIF3C. This could be because KAP either acts as an adaptor for other kinesins or serves some other function on these organelles. There is little evidence supporting this, as there are no other proposed functions of KAP. A second possible explanation is that the kinesin tail strategy could cause a dominant negative effect and reduce transport. However, the comparable velocities between KAP and KIF3AB/KIF3C suggests that the motor complexes are not substantially impaired in their ability to move organelles. Furthermore, previous experiments with kinesin tail constructs did not find any substantial change in the trafficking behavior of cargo-labeled vesicles (Jenkins *et al.*, 2012; Bentley and Banker, 2015; Yang *et al.*, 2019; Frank *et al.*, 2020; Montgomery *et al.*, 2022). A third interpretation is that KAP binding to organelles is more stable than KIF3AB or KIF3AC binding to KAP. If KAP mediates KIF3 binding to organelles, KAP detachment would also result in the loss of bound kinesins. In contrast, if kinesin–KAP interactions were severed, KAP could remain on moving organelles, even if the kinesin signal was lost. This model is consistent with the observation that KAP expression typically resulted in a higher signal-to-noise ratio for organelle labeling, with less cytoplasmic background. Furthermore, KAP can form a complex with endogenous kinesins, whereas expressed KIF3AB and KIF3AC rely on endogenous adaptors, likely KAP, to bind to organelles. It is clear from the dim fluorescent signal that a small number of kinesins and KAP bind to any given organelle at once. If kinesins cycle on and off organelles at a higher rate, it is plausible that fluorescent kinesins detach during movement. This is consistent with the larger number of moving KAP organelles we observed.

Overall, these results show that KIF3B, KIF3C, and KAP organelles displayed comparable transport parameters, size and morphology, and cellular distribution. The similarities in their distribution and their transport parameters suggest the hypothesis that some fraction of the organelles labeled by KIF3B, KIF3C, and KAP are identical.

KIF3AB, KIF3AC, and KAP bind the same neuronal organelle populations

To determine the amount of KIF3AB, KIF3AC, and KAP colocalization on the same organelles, we performed a series of two-color experiments (Figure 7). We expressed GFP-KIF3B tail with Halo-KAP (Figure 7A), GFP-KIF3C tail with Halo-KAP (Figure 7B), or GFP-KIF3B tail with Halo-KIF3C tail (Figure 7C), each coexpressed with untagged KIF3A. Halotags were visualized with JF549 before fixation and imaging. High-magnification images from representative dendrites show that there was overwhelming overlap in all three conditions. We quantified colocalization by measuring Pearson’s correlation coefficients in dendritic regions with organelles (Figure 7D). For cellular imaging data, no correlation typically results in Pearson’s correlation coefficients lower than 0.4. All three conditions resulted in coefficients of 0.8 or higher, indicating extraordinarily high colocalization. Together, these data indicate that KIF3B, KIF3C, and KAP bind the same organelle populations.

APC is a neuronal KIF3 cargo

Beyond IFT, little is known about neuronal KIF3 cargoes. The strongest evidence of a non-IFT cargo is APC, although this interaction is not well characterized in neurons (Jimbo *et al.*, 2002; Alsabban

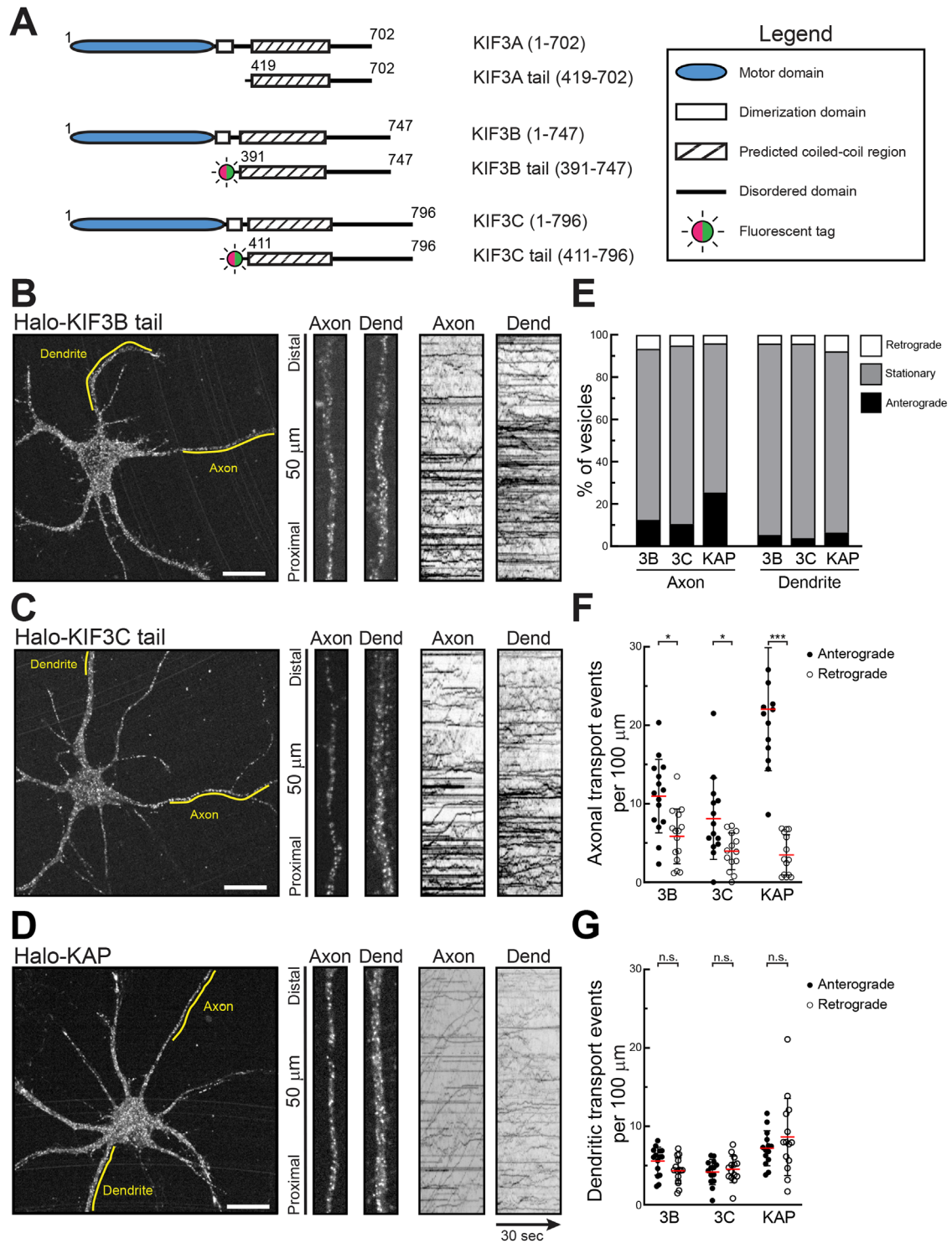


FIGURE 5: Characterization of KIF3B, KIF3C, and KAP organelles in cultured hippocampal neurons. (A) Schematic showing the construct design. (B–D) Representative images of 7 to 8 DIV hippocampal neurons expressing the indicated proteins. GFP-KIF3B and GFP-KIF3C were coexpressed with untagged KIF3A tail. Halotag was visualized with JF549. Yellow lines on each cell indicate sections of the axon and dendrite from which the high-magnification views and kymographs were generated. Scale bars: 20 μm . (E–G) Quantification of organelle motility and transport events. Sample sizes: KIF3B: 15 cells, 1027 axonal and 4741 dendritic organelles; KIF3C: 15 cells, 1090 axonal and 4747 dendritic organelles; KAP: 14 cells, 1001 axonal and 4470 dendritic organelles. * $p < 0.05$; *** $p < 0.001$.

et al., 2020; Baumann et al., 2020). There is also neuronal immunofluorescence evidence that KIF3C binds to organelles containing FMRP (Davidovic et al., 2007). Consistent colocalization of fluores-

cently tagged proteins, especially when colocalization remains stable for longer periods in live cells, is some of the strongest evidence that two proteins bind the same organelles. Because KIF3B and

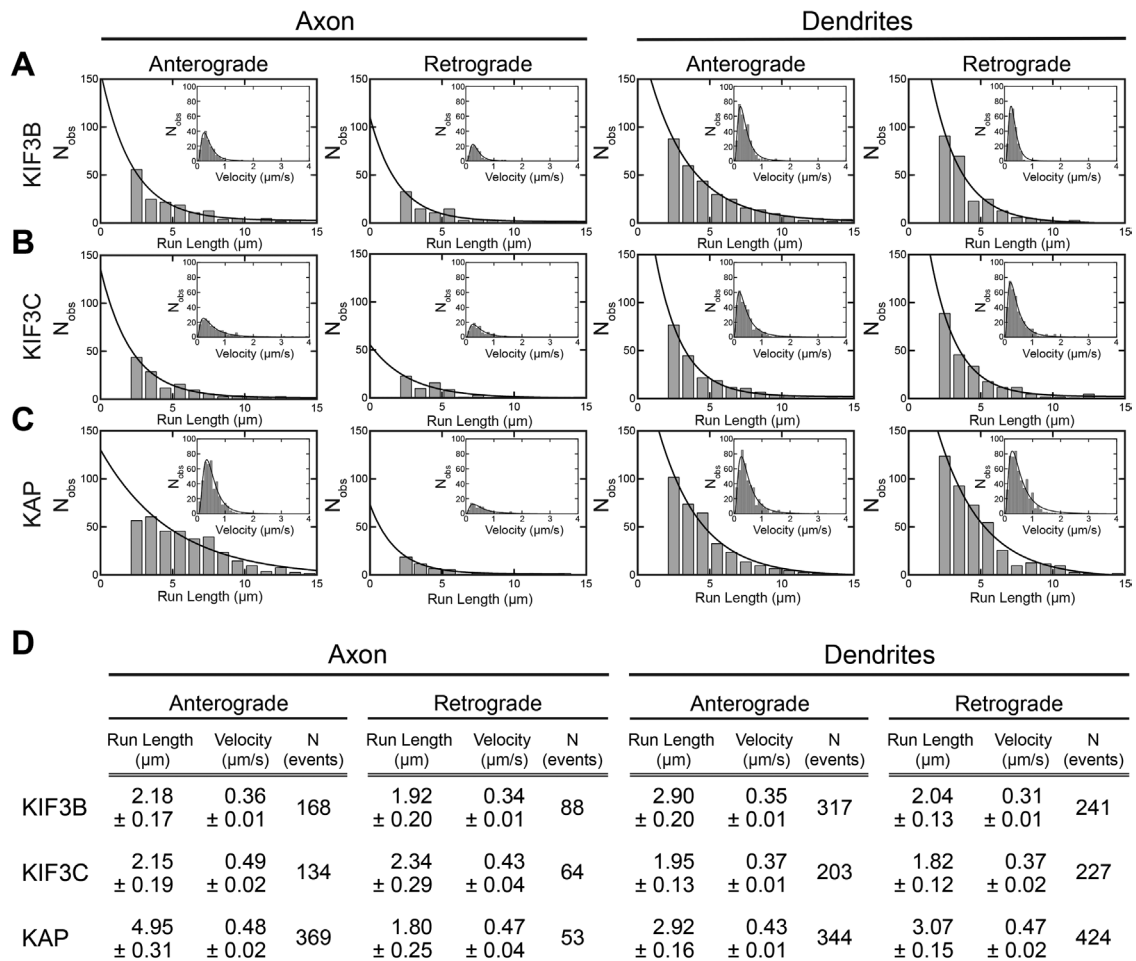


FIGURE 6: KIF3B, KIF3C, and KAP organelles exhibit comparable transport parameters. (A–C) Histograms showing the distribution of organelle run lengths and velocities with SEM. (D) Compiled transport parameters. Mean run length was generated by fitting to a single-exponential decay function. Cell sample sizes: KIF3B: 15; KIF3C: 14; KAP: 14.

KIF3C bind the same organelles, we chose KIF3C tail, which labeled organelles more consistently, and determined colocalization with fluorescently tagged APC and FMRP. We used the KIF5 cargo neuron-glia cell adhesion molecule (NgCAM; L1 in mammals) (Jareb and Banker, 1998; Sampo *et al.*, 2003; Lasiecka *et al.*, 2010; Hoo *et al.*, 2016; Yang *et al.*, 2019; Nabb and Bentley, 2022) as a baseline for incidental colocalization. We expressed Halo-KIF3C (visualized with JF549) and unlabeled KIF3A tails with APC-mEmerald, GFP-FMRP, or NgCAM-GFP (Figure 8, A–C). High-magnification images show that APC colocalized with KIF3C (Figure 8A). In contrast, KIF3C did not colocalize with FMRP or NgCAM (Figure 8, B and C). We quantified the percentage of KIF3C organelles colocalized with each cargo as well as the percentage of cargo that colocalized with KIF3C (Figure 8D). About 12% of KIF3C structures colocalized with APC in axons and dendrites. KIF3C rarely colocalized with FMRP and NgCAM. Therefore, APC is a likely KIF3 cargo. These results also suggest that, despite previous data, FMRP is likely not a KIF3AC cargo in hippocampal neurons. The quantification also indicates that KIF3 binds to cargoes other than APC that are not yet identified.

DISCUSSION

This study addresses the function of heterodimeric Kinesin-2 family members KIF3A, KIF3B, and KIF3C in mammalian neurons. We developed a microscopy-based strategy to determine protein–protein interactions in intact neurons. With this assay, we found that KIF3AB

and KIF3AC both bound KAP and that KAP recognizes the C-terminal disordered domain of KIF3s. We also refined a strategy to visualize organelle-bound KIF3AB, KIF3AC, and KAP and used that approach to generate live-cell recordings to measure the transport parameters of these organelles and to identify neuronal cargoes. KIF3/KAP organelles were mostly stationary but underwent sporadic transport, and all bind the same organelle population. Part of this population are APC-positive organelles. However, APC accounted for only ~12% of KIF3 organelles, indicating the existence of other cargoes. This systematic study defines the parameters of KIF3/KAP organelles in neurons and provides the tools for future work that will identify additional KIF3/KAP cargoes and determine the regulatory mechanisms of organelle-bound KIF3/KAP.

The KIF3/KAP complex

We found that the KIF3AB/KAP complex assembles in neurons and binds organelles outside of IFT. Previous studies proposed a non-IFT function for KIF3AB in neurons, but to date there has been no evidence showing organelle-bound KIF3AB in live neurons (Takeda *et al.*, 2000; Teng *et al.*, 2005; Ichinose *et al.*, 2015, 2019; Alsabban *et al.*, 2020; Joseph *et al.*, 2020). It is well-established that KIF3AB forms a complex with KAP in IFT. However, the structure of the assembled complex is not well defined. Early electron micrographs of KIF3AB/KAP suggested that KAP binds the C-terminal disordered domain of KIF3AB (Wedaman *et al.*, 1996; Yamazaki *et al.*, 1996). In

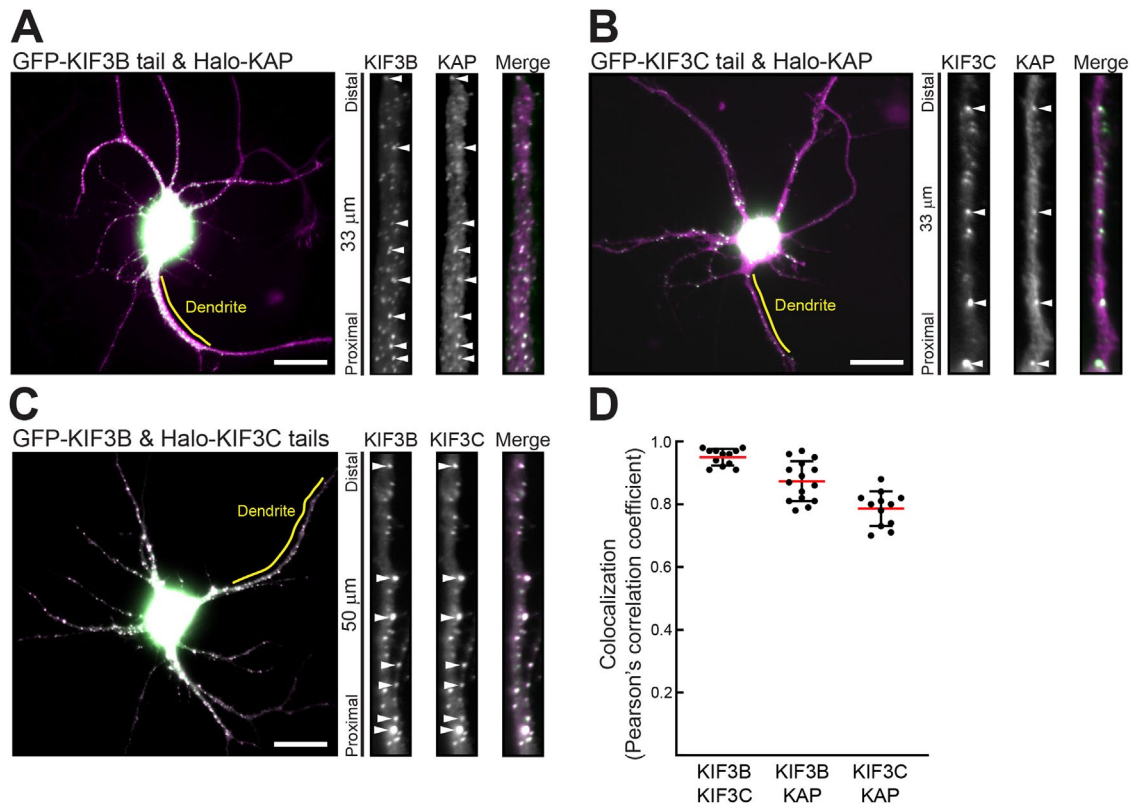


FIGURE 7: KIF3B, KIF3C, and KAP bind the same neuronal organelle populations. (A–C) Representative images of 7 to 9 DIV hippocampal neurons expressing the indicated constructs. KIF3B and KIF3C were coexpressed with untagged KIF3A tail. Yellow lines indicate regions from which high-magnification views were generated. Arrowheads point to examples of colocalization. Scale bar: 20 μm. (D) Quantification of colocalization of the indicated proteins. Cell sample sizes: KIF3B/KIF3C: 12; KIF3B/KAP: 15; KIF3C/KAP: 12.

contrast, biochemical analysis of interactions between heterodimeric Kinesin-2 and KAP in *Drosophila* found that KAP recognized the KIF3 coiled-coil domains (Doodhi *et al.*, 2009; Ahmed *et al.*, 2020). Purification of KAP for crystallography is difficult, and as a result, the structure of KIF3AB/KAP remains unsolved. We found that the C-terminal disordered domains of KIF3AB are sufficient for binding KAP, indicating that there are substantial differences in complex assembly between mammals and *Drosophila*. The clear result that the C-terminal domains of KIF3AB bind KAP may enable future studies to solve the structure of the KIF3AB/KAP and KIF3AC/KAP complexes.

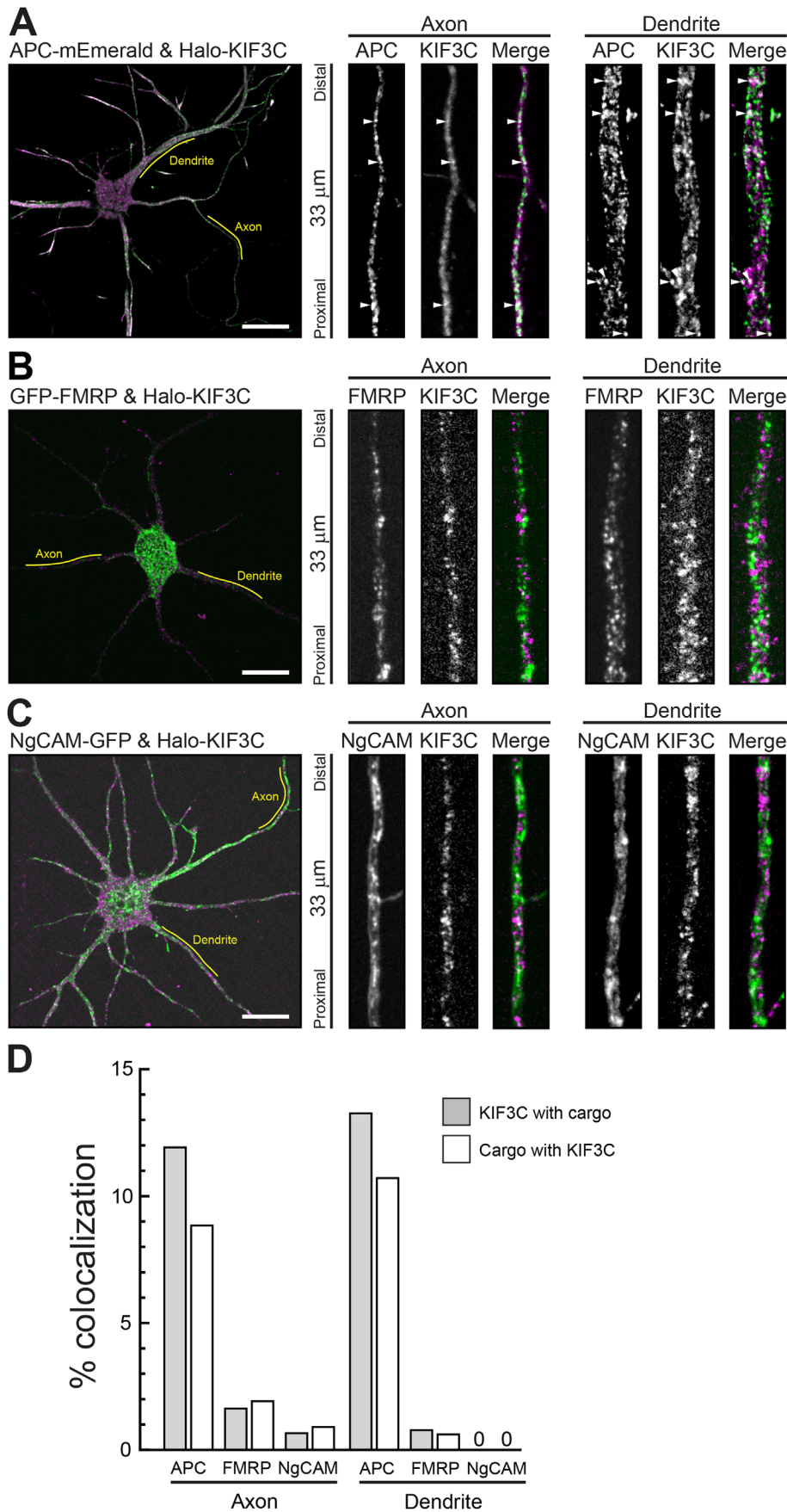
A second key discovery of this study is that KIF3AC binds KAP. This interaction is mediated by the C-terminal disordered domain, analogous to the interaction between KIF3AB and KAP. Recent experiments finding that KIF3AC cannot replace KIF3AB in the IFT KIF3/KAP complex (Engelke *et al.*, 2019) suggested that KIF3AC/KAP may not assemble, despite some biochemical evidence to the contrary (Yang and Goldstein, 1998). By showing that KIF3AC binds KAP and that KIF3C and KAP colocalize on the same organelles, our experiments resolve this seeming contradiction. Therefore, the difference between KIF3/KAP-mediated IFT and organelle transport is not due to differences in the abilities of KIF3B and KIF3C to bind KAP.

The neuronal function of KIF3/KAP

The systematic visualization of organelle-bound KIF3B, KIF3C, and KAP allowed us to quantify the trafficking behavior of KIF3/KAP cargoes and compare their “transport signature” to those of other kinesins. Compared to other transport vesicles, KIF3/KAP organelles

moved relatively infrequently. The moving KIF3/KAP organelles exhibited velocities of 0.3–0.5 μm/s, which is slower than those of organelles moved by Kinesin-1 or Kinesin-3 (Fu and Holzbaaur, 2013; Farfel-Becker *et al.*, 2019; Yang *et al.*, 2019; De Pace *et al.*, 2020; Frank *et al.*, 2020; Nabb and Bentley, 2022), but comparable to velocities of single KIF3AB and KIF3AC motors *in vitro* (Brunnbauer *et al.*, 2010; Pan *et al.*, 2010; Andreasson *et al.*, 2015; Guzik-Lendrum *et al.*, 2015; Baumann *et al.*, 2020) and during IFT in cilia (Broekhuis *et al.*, 2014; Engelke *et al.*, 2019). These parameters indicate that KIF3/KAP motors fulfill a specialized neuronal function that differs from that of other transport kinesins.

The observed trafficking behaviors are consistent with at least two functions that are not mutually exclusive. First, KIF3/KAP could act as a tether to stably maintain organelle position within neurons. The hypothesis that kinesins act as tethers is not a novel concept (Sheetz, 1987), but few examples have been described to date (Barlan and Gelfand, 2017), likely because most kinesin-related studies (including many of our own) focus on long-range transport. Microtubules in neuronal dendrites are structurally well suited for kinesin to act as tethers. Dendritic microtubules have an antiparallel organization (Baas *et al.*, 1988; Tas *et al.*, 2017; Weiner *et al.*, 2021). This orientation may enable microtubule plus end-directed KIF3/KAP engaged with antiparallel microtubules to create counteracting forces that maintain organelle positioning. A second mechanism may be that inactive KIF3/KAP binds organelles until an external signal triggers activation. The mechanisms of on-vesicle kinesin regulation are an emerging frontier in kinesin biology (Verhey and Hammond, 2009; Maday *et al.*, 2014; Cason and Holzbaaur, 2022;



Kumari and Ray, 2022; Nabb and Bentley, 2022). Kinesin autoinhibition was first described for Kinesin-1 (Verhey *et al.*, 1998) and is thought to be a regulatory mechanism for most—if not all—transport kinesins (Verhey and Hammond, 2009; Verhey *et al.*, 2011; Fu and Holzbaur, 2013; Bianchi *et al.*, 2016; Ren *et al.*, 2018; Twelvetrees *et al.*, 2019; Twelvetrees, 2020; Keren-Kaplan and Bonifacino, 2021; Chiba *et al.*, 2022), including heterodimeric Kinesin-2 (Hammond *et al.*, 2010). The mechanism by which organelle-bound KIF3/KAP is activated in neurons will be the subject of future studies.

A key finding of the study was that KIF3AB and KIF3AC both bind KAP and localize to the same neuronal organelles. This was somewhat surprising, as KIF3AB and KIF3AC are not redundant in IFT, where KIF3C cannot compensate for a loss of KIF3B (Engelke *et al.*, 2019). In contrast to IFT, little is known about the neuronal cargoes of KIF3/KAP. Previous studies using *in vitro* reconstitution (Baumann *et al.*, 2020) and immunofluorescence (Alsabban *et al.*, 2020) proposed APC as a KIF3AB/KAP cargo. We found robust colocalization of KIF3/KAP and APC. However, fewer than 15% of KIF3C organelles colocalized with APC, suggesting that most KIF3/KAP organelles have a different molecular identity. Interference with KIF3/KAP causes dysfunction or mislocalization of structural plasma membrane proteins (Teng *et al.*, 2005; Ichinose *et al.*, 2015; Soda *et al.*, 2022) and *N*-methyl-D-aspartate receptors (Alsabban *et al.*, 2020), although the causal link of these interactions is not yet fully established.

Finally, KIF3/KAP organelles may function as signaling hubs that regulate neuronal development (Huangfu *et al.*, 2003; Nishimura *et al.*, 2004; Ichinose *et al.*, 2019). KIF3/KAP is thought to localize several proteins during neuronal development to the

FIGURE 8: KIF3/KAP colocalizes with APC and not FMRP or NgCAM. (A–C) Representative images of 6 to 9 DIV hippocampal neurons expressing the indicated constructs and untagged KIF3A tail. Halotags were visualized with JF549. Yellow lines indicate regions from which high-magnification views were generated. Arrowheads highlight examples of colocalization. Scale bars: 20 μ m. (D) Quantification of colocalization between KIF3C and the indicated cargoes. Cell sample sizes: APC: 17; FMRP: 10; NgCAM: 10.

axon. For example, KIF3/KAP localizes the kinase Par3 to the axon of stage 3 neurons, potentially to generate a local signaling hub that aids axon outgrowth (Nishimura *et al.*, 2004). During axon formation, KIF3/KAP localizes TRIM46 to the proximal axon, where TRIM46 stabilizes parallel microtubules, aiding axon formation. However, the specific molecular mechanism by which KIF3/KAP localizes these proteins during development are not yet defined. The tools developed here expand the experimental repertoire for future studies that address the role of KIF3/KAP in neuronal development and maintenance.

A novel assay to determine protein–protein interactions in intact neurons

To determine KIF3/KAP interactions in neurons, we developed a microscopy-based protein–protein binding assay. This approach ensures that cell type-specific accessory proteins are present. This is particularly relevant for neurons, a highly specialized cell type (Arendt *et al.*, 2016, 2019; Bentley and Banker, 2016; Yogev and Shen, 2017). Traditional coimmunoprecipitation experiments often use non-neuronal cell types to generate sufficient protein material for biochemistry. Such experiments also rely on careful buffer calibration, as salt level and pH drastically impact protein binding. Conducting the experiment in intact neurons circumvents these problems and enables the analysis of binding interactions in the proteins' native milieu, the cytoplasm. It also allows for multiple, relatively easy experimental replicates, as each cell functionally acts as an independent experiment.

As with any assay, proper application requires caution. Most crucially for primary neurons, interpretable experiments require cultures of consistent and high quality. This is particularly important for any colocalization experiments, as sporadic colocalization and aggregates formation tend to be increased in dying cells. Targeting the candidate protein to peroxisomes with the FRB-FKBP heterodimerization system addresses this concern because it ensures that colocalization is specific and not an artifact of unhealthy cell cultures. Combined with quantitative analysis, this assay is a convenient tool for confidently defining protein–protein interactions in neurons.

MATERIALS AND METHODS

Cell culture

Primary hippocampal neuronal cultures were prepared as previously described (Kaech and Banker, 2006; Kaech *et al.*, 2012; Frank *et al.*, 2020; Nabb and Bentley, 2022). In brief, hippocampi from E18 rats were dissected, trypsinized, dissociated, and plated on 18 mm poly-L-lysine-treated glass coverslips. Minimum essential medium with N2 supplements was used to grow cultures in a 37°C incubator with 5% CO₂. Six to 10 days in vitro (DIV) neurons were transfected with expression constructs and Lipofectamine 2000 (Thermo Fisher). For imaging KIF3/KAP organelles, constructs were expressed for about 3–7 h to minimize the cytosolic pool. For coexpression with candidate cargo proteins, constructs were expressed for 8–24 h to facilitate robust cargo labeling. APC required long (12+ h) expression to be visualized, likely due to its large size (2843 residues, 310 kDa). For protein–protein binding experiments requiring expression of multiple constructs, cells were fixed after overnight expression.

DNA constructs

Construct details are given in Table 1. Kinesin tail construct design was previously described (Yang *et al.*, 2019). In short, kinesin tails were designed to exclude the N-terminus containing the motor domain up to and including the first predicted coiled-coil dimerization domain (defined by EMBnet [<https://bio.tools/coils>]).

Imaging

Live-cell recordings were acquired with an Andor Dragonfly built on a Nikon Ti2 with a CFI Apo 60× 1.49 objective and two sCMOS cameras (Zyla 4.2+; Andor). The imaging stage, microscope objective, and sample were maintained at 37°C in a full lexan incubation ensemble (OkoLab). The z-axis movement was controlled by a Perfect Focus System. During imaging, neurons were maintained in Hibernate E without phenol red (BrainBits). Images were acquired at 2 frames per second for 30 s. Axons were identified with an anti-neurofascin antibody (NeuroMab Cat#75-027) conjugated to CF405 (Mix-n-Stain CF405S antibody labeling kit; Biotum Cat#92231) in the imaging medium.

For fixed-cell recordings, neurons were fixed with 4% paraformaldehyde/4% sucrose in phosphate-buffered saline for 20 min at 37°C. Coverslips were mounted on slides with ProLong Diamond Anti-fade (Thermo Fisher Cat#P36961). Fixed cell images were recorded with a Zeiss Axio Imager Z1 microscope equipped with a 63× 1.4 Plan-Apochromat objective and a charge-coupled device (AxioCam 506 mono; Zeiss).

Halotag-expressing cells were incubated with 50 nM JF549 or JF646 (Grimm *et al.*, 2015) for 5 min and washed with conditioned medium for 5 min before imaging or fixation. For protein–protein binding assays, neurons were incubated with 100 nM linker (AP21967; Takara Cat#635056) for 2 h before fixation.

Analysis

All analysis was performed by a single blinded reviewer. To ensure consistency and reduce bias, multiple experiments were combined into a large data set and the analyst was blinded to the condition.

Kymographs were generated with MetaMorph software (Molecular Devices). A single analyst manually identified all transport events from kymographs. Each continuous line with a constant slope was scored as a single transport event. A single organelle could undergo multiple transport events if there was a distinct pause (>3 frames) between them. Event coordinates were exported to Microsoft Excel or GraphPad Prism for statistical analysis. To ensure that only microtubule-based, long-range transport events were included in the analysis, excursions <2 μm were excluded. Run length and velocities were calculated with 1 μm bin size and a 0.1 μm/s bin sizes, respectively. Mean run lengths were calculated using a single exponential decay following the equation

$$y = y_0 + A \left(\frac{-x}{T} \right)$$

where A is the maximum amplitude and T is the mean run length reported as \pm SEM.

The velocity was curve fitted to a log-normal distribution, following the equation

$$y = \frac{1}{\sigma\sqrt{2\pi}} e^{-(x-\mu)^2/(2\sigma^2)}$$

where $\mu \in (-\infty, +\infty)$ and $\sigma > 0$, and the geometric mean following the equation

$$\exp\left(\mu + \frac{\sigma^2}{2}\right)$$

The numbers of stationary, moving, and total organelles were generated by kymograph analysis and by manual counting in the same regions of axons and dendrites from which the kymographs were generated. These values were used to calculate the percent of moving and stationary organelles.

Construct	Construct design	Accession number	Source
FRB-KIF3A tail	FRB-3myc-GGGSGGGSGGGLYK-KIF3A ⁴¹⁹⁻⁷⁰²	NM_001300792.1 variant 2	Yang <i>et al.</i> , 2019
GFP-KIF3A tail	GFP-GGGSGGGSGGGLYK-KIF3A ⁴¹⁹⁻⁷⁰²	NM_001300792.1 variant 2	This paper
Halo-KIF3A tail	Halotag-LYGGSGGGSGGGLYK-KIF3A ⁴¹⁹⁻⁷⁰²	NM_001300792.1 variant 2	This paper
GFP-KIF3A ^{CC}	GFP-GGGSGGGSGGGLYK-KIF3A ⁴¹⁹⁻⁵⁸⁹	NM_001300792.1 variant 2	This paper
Halo-KIF3A ^{CC}	Halotag-LYGGSGGGSGGGLYK-KIF3A ⁴¹⁹⁻⁵⁸⁹	NM_001300792.1 variant 2	This paper
GFP-KIF3A ^{DD}	GFP-GGGSGGGSGGGLYI-KIF3A ⁵⁹⁰⁻⁷⁰²	NM_001300792.1 variant 2	This paper
Halo-KIF3A ^{DD}	Halotag-LYGGSGGGSGGGLYI-KIF3A ⁵⁹⁰⁻⁷⁰²	NM_001300792.1 variant 2	This paper
GFP-KIF3B tail	GFP-GGGSGGGSGGGLYK-KIF3B ³⁹¹⁻⁷⁴⁷	NM_008444.4	Yang <i>et al.</i> , 2019
Halo-KIF3B tail	Halotag-LYGGSGGGSGGGLYK-KIF3B ³⁹¹⁻⁷⁴⁷	NM_008444.4	This paper
GFP-KIF3B ^{CC}	GFP-GGGSGGGSGGGLYK-KIF3B ³⁹¹⁻⁵⁹²	NM_008444.4	This paper
Halo-KIF3B ^{CC}	Halotag-LYGGSGGGSGGGLYK-KIF3B ³⁹¹⁻⁵⁹²	NM_008444.4	This paper
GFP-KIF3B ^{DD}	GFP-GGGSGGGSGGGLYK-KIF3B ⁵⁹³⁻⁷⁴⁷	NM_008444.4	This paper
Halo-KIF3B ^{DD}	Halotag-LYGGSGGGSGGGLYK-KIF3B ⁵⁹³⁻⁷⁴⁷	NM_008444.4	This paper
GFP-KIF3C tail	GFP-GGGSGGGSGGGLYR-KIF3C ⁴¹¹⁻⁷⁹⁶	NM_008445.2	Yang <i>et al.</i> , 2019
Halo-KIF3C tail	Halotag-LYGGSGGGSGGGLYR-KIF3C ⁴¹¹⁻⁷⁹⁶	NM_008445.2	This paper
GFP-KIF3C ^{CC}	GFP-GGGSGGGSGGGLYR-KIF3C ⁴¹¹⁻⁶¹⁵	NM_008445.2	This paper
Halo-KIF3C ^{CC}	Halotag-LYGGSGGGSGGGLYR-KIF3C ⁴¹¹⁻⁶¹⁵	NM_008445.2	This paper
GFP-KIF3C ^{DD}	GFP-GGGSGGGSGGGLYT-KIF3C ⁶¹⁶⁻⁷⁹⁶	NM_008445.2	This paper
Halo-KIF3C ^{DD}	Halotag-LYGGSGGGSGGGLYT-KIF3C ⁶¹⁶⁻⁷⁹⁶	NM_008445.2	This paper
FRB-KAP	FRB-3myc-GGGSGGGSGGGLYK-KAP3B	NM_001375831.1	This paper
Halo-KAP	Halotag-LYGGSGGGSGGGLYK-KAP3B	NM_001375831.1	This paper
GFP-KIF5C tail	GFP-GGGSGGGSGGGLYKGGSGGGSGGSP-KIF5C ³⁷⁸⁻⁹⁵⁵	NM_001107730	Yang <i>et al.</i> , 2019
PEX3-tdTomato-FKBP	PEX3-GGSGSGGPRPT-tdTomato-RTGASGGSGGGSGGGSGGTR-FKBP	NM_003630.3	This paper
APC-mEmerald	APC-FGGSAASGSADPPVAT-mEmerald	NM_000038.6	Adapted from Morin <i>et al.</i> , 1997
GFP-FMRP	GFP-SGLRSRAQASNSMEDYKDDDDK-FMRP	NM_002024.6	Adapted from Stetler <i>et al.</i> , 2006
NgCAM-GFP	NgCAM-KLGAAPRPT-GFP	NM_205153.1	Nabb and Bentley, 2022

TABLE 1: Expression constructs.

To calculate the Pearson's correlation coefficients for protein-protein binding experiments (Figures 1–4), three to five clustered and brightly labeled peroxisomes were identified in a dendrite. A region of interest was drawn around these peroxisomes, and the Pearson's correlation coefficient was calculated with the Coloc2 FIJI plug-in.

For KIF3 organelle colocalization (Figure 7), Pearson's correlation coefficients were generated from representative dendrites of each neuron.

The percent colocalization of KIF3C with cargoes (Figure 8) was calculated by manual counting of fluorescent structures in both channels. Organelles were classified as "not colocalized" and "colocalized with comparable morphology."

P values for Pearson's correlation coefficients were determined by Student's *t* test. Error bars show the SEM.

ACKNOWLEDGMENTS

We thank Geraldine Quinones for excellent technical assistance in culturing and maintaining hippocampal neurons. We thank Jasper Jeffrey for help with figure design. We thank the BioResearch facility at Rensselaer for assistance with husbandry and tissue collection. Research reported in this publication was supported by National Institute of Mental Health award R01MH066179 to M.B., National

Institute of General Medical Sciences (NIGMS) award R37GM054141 to S.P.G., and a NIGMS Training Program T32GM067545 pre-doctoral fellowship to A.G. The content is solely the responsibility of the authors and does not necessarily represent the official views of the National Institutes of Health.

REFERENCES

- Ahmed Z, Mazumdar S, Ray K (2020). Kinesin associated protein, DmKAP, binding harnesses the C-terminal ends of the *Drosophila* kinesin-2 stalk heterodimer. *Biochem Biophys Res Commun* 522, 506–511.
- Alsabban AH, Morikawa M, Tanaka Y, Takei Y, Hirokawa N (2020). Kinesin Kif3b mutation reduces NMDAR subunit NR 2A trafficking and causes schizophrenia-like phenotypes in mice. *EMBO J* 39, 1–19.
- Andreasson JOL, Shastry S, Hancock WO, Block SM (2015). The mechanochemical cycle of mammalian kinesin-2 KIF3A/B under load. *Curr Biol* 25, 1166–1175.
- Arendt D, Bertucci PY, Achim K, Musser JM (2019). Evolution of neuronal types and families. *Curr Opin Neurobiol* 56, 144–152.
- Arendt D, Musser JM, Baker CVH, Bergman A, Cepko C, Erwin DH, Pavlicev M, Schlosser G, Widder S, Laubichler MD, *et al.* (2016). The origin and evolution of cell types. *Nat Rev Genet* 17, 744–757.
- Baas PW, Deitch JS, Black MM, Banker GA (1988). Polarity orientation of microtubules in hippocampal neurons: uniformity in the axon and non-uniformity in the dendrite. *Proc Natl Acad Sci USA* 85, 8335–8339.
- Banaszynski LA, Liu CW, Wandless TJ (2005). Characterization of the FKBP-rapamycin-FRB ternary complex. *J Am Chem Soc* 127, 4715–4721.

- Barlan K, Gelfand VI (2017). Microtubule-based transport and the distribution, tethering, and organization of organelles. *Cold Spring Harb Perspect Biol* 9, a025817.
- Baumann S, Komissarov A, Gili M, Ruprecht V, Wieser S, Maurer SP (2020). A reconstituted mammalian APC-kinesin complex selectively transports defined packages of axonal mRNAs. *Sci Adv* 6, eaaz1588.
- Belshaw PJ, Ho SN, Crabtree GR, Schreiber SL (1996). Controlling protein association and subcellular localization with a synthetic ligand that induces heterodimerization of proteins. *Proc Natl Acad Sci USA* 93, 4604–4607.
- Bensel BM, Guzik-Lendrum S, Masucci EM, Woll KA, Eckenhoff RG, Gilbert SP (2017). Common general anesthetic propofol impairs kinesin processivity. *Proc Natl Acad Sci USA* 114, E4281–E4287.
- Bentley M, Banker G (2015). A novel assay to identify the trafficking proteins that bind to specific vesicle populations. *Curr Protoc Cell Biol* 69, 13.8.1–13.8.12.
- Bentley M, Banker G (2016). The cellular mechanisms that maintain neuronal polarity. *Nat Rev Neurosci* 17, 611–622.
- Bentley M, Decker H, Luisi J, Banker G (2015). A novel assay reveals preferential binding between rabs, kinesins, and specific endosomal subpopulations. *J Cell Biol* 208, 273–281.
- Bianchi S, Van Riel WE, Kraatz SHW, Olieric N, Frey D, Katrukha EA, Jaussi R, Missimer J, Grigoriev I, Olieric V, et al. (2016). Structural basis for misregulation of kinesin KIF21A autoinhibition by CFEOM1 disease mutations. *Sci Rep* 6, 1–16.
- Bodakuntla S, Schnitzler A, Villablanca C, Gonzalez-Billault C, Bieche I, Janke C, Magiera MM (2020). Tubulin polyglutamylation is a general traffic control mechanism in hippocampal neurons. *J Cell Sci* 133, jcs241802.
- Broekhuis JR, Verhey KJ, Jansen G (2014). Regulation of cilium length and intraflagellar transport by the RCK-kinases ICK and MOK in renal epithelial cells. *PLoS One* 9, e108470.
- Brunnbauer M, Mueller-Planitz F, Kösem S, Ho TH, Dombi R, Gebhardt JCM, Rief M, Ökten Z (2010). Regulation of a heterodimeric kinesin-2 through an unprocessive motor domain that is turned processive by its partner. *Proc Natl Acad Sci USA* 107, 10460–10465.
- Burack MA, Silverman MA, Banker G (2000). The role of selective transport in neuronal protein sorting. *Neuron* 26, 465–472.
- Carpenter BS, Barry RL, Verhey KJ, Allen BL (2015). The heterotrimeric kinesin-2 complex interacts with and regulates GLI protein function. *J Cell Sci* 128, 1034–1050.
- Cason SE, Holzbaaur ELF (2022). Selective motor activation in organelle transport along axons. *Nat Rev Mol Cell Biol*, doi:10.1038/s41580-022-00491-w.
- Chiba K, Ori-McKenney KM, Niwa S, McKenney RJ (2022). Synergistic autoinhibition and activation mechanisms control kinesin-1 motor activity. *Cell Rep* 39, 110900.
- Davidovic L, Jaglin XH, Lepagnol-Bestel AM, Tremblay S, Simonneau M, Bardoni B, Khandjian EW (2007). The fragile X mental retardation protein is a molecular adaptor between the neurospecific KIF3C kinesin and dendritic RNA granules. *Hum Mol Genet* 16, 3047–3058.
- Delorenzi M, Speed T (2002). An HMM model for coiled-coil domains and a comparison with PSSM-based predictions. *Bioinformatics* 18, 617–625.
- De Pace R, Britt DJ, Mercurio J, Foster AM, Djavaherian L, Hoffmann V, Abebe D, Bonifacio JS (2020). Synaptic vesicle precursors and lysosomes are transported by different mechanisms in the axon of mammalian neurons. *Cell Rep* 31, 107775.
- Doodhi H, Ghosal D, Krishnamurthy M, Jana SC, Shamala D, Bhaduri A, Sowdhamini R, Ray K (2009). KAP, the accessory subunit of kinesin-2, binds the predicted coiled-coil stalk of the motor subunits. *Biochemistry* 48, 2248–2260.
- Encell LP (2012). Development of a dehalogenase-based protein fusion tag capable of rapid, selective and covalent attachment to customizable ligands. *Curr Chem Genomics* 6, 55–71.
- Engelke MF, Waas B, Kearns SE, Suber A, Boss A, Allen BL, Verhey KJ (2019). Acute inhibition of heterotrimeric kinesin-2 function reveals mechanisms of intraflagellar transport in mammalian cilia. *Curr Biol* 29, 1137–1148.e4.
- Farfel-Becker T, Roney JC, Cheng XT, Li S, Cuddy SR, Sheng ZH (2019). Neuronal soma-derived degradative lysosomes are continuously delivered to distal axons to maintain local degradation capacity. *Cell Rep* 28, 51–64.e4.
- Frank M, Citarella CG, Quinones GB, Bentley M (2020). A novel labeling strategy reveals that myosin Va and myosin Vb bind the same dendritically polarized vesicle population. *Traffic* 21, 689–701.
- Fu MM, Holzbaaur ELF (2013). JIP1 regulates the directionality of APP axonal transport by coordinating kinesin and dynein motors. *J Cell Biol* 202, 495–508.
- Funabashi T, Katoh Y, Okazaki M, Sugawa M, Nakayama K (2018). Interaction of heterotrimeric kinesin-II with IFT-B-connecting tetramer is crucial for ciliogenesis. *J Cell Biol* 217, 2867–2876.
- Gilbert SP, Guzik-Lendrum S, Rayment I (2018). Kinesin-2 motors: kinetics and biophysics. *J Biol Chem* 293, 4510–4518.
- Grimm JB, English BP, Chen J, Slaughter JP, Zhang Z, Revyakin A, Patel R, Macklin JJ, Normanno D, Singer RH, et al. (2015). A general method to improve fluorophores for live-cell and single-molecule microscopy. *Nat Methods* 12, 244–250.
- Gumy LF, Chew DJ, Tortosa E, Katrukha EA, Kapitein LC, Tolkovsky AM, Hoogenraad CC, Fawcett JW (2013). The kinesin-2 family member KIF3C regulates microtubule dynamics and is required for axon growth and regeneration. *J Neurosci* 33, 11329–11345.
- Guzik-Lendrum S, Rank KC, Bensel BM, Taylor KC, Rayment I, Gilbert SP (2015). Kinesin-2 KIF3AC and KIF3AB can drive long-range transport along microtubules. *Biophys J* 109, 1472–1482.
- Guzik-Lendrum S, Rayment I, Gilbert SP (2017). Homodimeric kinesin-2 KIF3CC promotes microtubule dynamics. *Biophys J* 113, 1845–1857.
- Hackney DD, Levitt JD, Wagner DD (1991). Characterization of alpha 2 beta 2 and alpha 2 forms of kinesin. *Biochem Biophys Res Commun* 174, 810–815.
- Hammond JW, Blasius TL, Soppina V, Cai D, Verhey KJ (2010). Autoinhibition of the kinesin-2 motor KIF17 via dual intramolecular mechanisms. *J Cell Biol* 189, 1013–1025.
- Hoo LS, Banna CD, Radeke CM, Sharma N, Albertolle ME, Low SH, Weimbs T, Vandenberg CA (2016). The SNARE protein syntaxin 3 confers specificity for polarized axonal trafficking in neurons. *PLoS One* 11, 1–20.
- Huang C, Banker G (2012). The translocation selectivity of the kinesins that mediate neuronal organelle transport. *Traffic* 13, 549–564.
- Huangfu D, Liu A, Rakeman AS, Murcia NS, Niswander L, Anderson KV (2003). Hedgehog signalling in the mouse requires intraflagellar transport proteins. *Nature* 426, 83–87.
- Ichinose S, Ogawa T, Hirokawa N (2015). Mechanism of activity-dependent cargo loading via the phosphorylation of KIF3A by PKA and CaMKIIa. *Neuron* 87, 1022–1035.
- Ichinose S, Ogawa T, Jiang X, Hirokawa N (2019). The spatiotemporal construction of the axon initial segment via KIF3/KAP3/TRIM46 transport under MARK2 signaling. *Cell Rep* 28, 2413–2426.e7.
- Jareb M, Banker G (1998). The polarized sorting of membrane proteins expressed in cultured hippocampal neurons using viral vectors. *Neuron* 20, 855–867.
- Jenkins B, Decker H, Bentley M, Luisi J, Banker G (2012). A novel split kinesin assay identifies motor proteins that interact with distinct vesicle populations. *J Cell Biol* 198, 749–761.
- Jimbo T, Kawasaki Y, Koyama R, Sato R, Takada S, Haraguchi K, Akiyama T (2002). Identification of a link between the tumour suppressor APC and the kinesin superfamily. *Nat Cell Biol* 4, 323–327.
- Joseph NF, Grinman E, Swarnkar S, Puthanveetil SV (2020). Molecular motor KIF3B acts as a key regulator of dendritic architecture in cortical neurons. *Front Cell Neurosci* 14, 521199.
- Kaech S, Banker G (2006). Culturing hippocampal neurons. *Nat Protoc* 1, 2406–2415.
- Kaech S, Huang C-F, Banker G (2012). General considerations for live imaging of developing hippocampal neurons in culture. *Cold Spring Harb Protoc* 2012, 312–318.
- Kapitein LC, Schlager MA, Kuijpers M, Wulf PS, van Spronsen M, MacKintosh FC, Hoogenraad CC (2010). Mixed microtubules steer dynein-driven cargo transport into dendrites. *Curr Biol* 20, 290–299.
- Keren-Kaplan T, Bonifacio JS (2021). ARL8 relieves SKIP autoinhibition to enable coupling of lysosomes to kinesin-1. *Curr Biol* 31, 540–554.e5.
- Kondo S, Sato-Yoshitake R, Noda Y, Aizawa H, Nakata T, Matsuura Y, Hirokawa N (1994). KIF3A is a new microtubule-based anterograde motor in the nerve axon. *J Cell Biol* 125, 1095–1107.
- Koppers M, Farias GG (2021). Organelle distribution in neurons: logistics behind polarized transport. *Curr Opin Cell Biol* 71, 46–54.
- Kumari D, Ray K (2022). Phosphoregulation of kinesins involved in long-range intracellular transport. *Front Cell Dev Biol* 10, 873164.
- Lasiecka ZM, Yap CC, Caplan S, Winckler B (2010). Neuronal early endosomes require EHD1 for L1/NgCAM trafficking. *J Neurosci* 30, 16485–16497.
- Lewis TR, Kundinger SR, Link BA, Insinna C, Besharse JC (2018). Kif17 phosphorylation regulates photoreceptor outer segment turnover. *BMC Cell Biol* 19, 25.
- Lo KY, Kuzmin A, Unger SM, Petersen JD, Silverman MA (2011). KIF1A is the primary anterograde motor protein required for the axonal transport

- of dense-core vesicles in cultured hippocampal neurons. *Neurosci Lett* 491, 168–173.
- Los GV, Encell LP, McDougall MG, Hartzell DD, Karassina N, Zimprich C, Wood MG, Learish R, Ohana RF, Urh M, et al. (2008). HaloTag: a novel protein labeling technology for cell imaging and protein analysis. *ACS Chem Biol* 3, 373–382.
- Maday S, Twelvetrees AE, Moughamian AJ, Holzbaur ELF (2014). Axonal transport: cargo specific mechanisms of motility and regulation. *Neuron* 84, 292–309.
- Milic B, Andreasson JOL, Hogan DW, Block SM (2017). Intraflagellar transport velocity is governed by the number of active KIF17 and KIF3AB motors and their motility properties under load. *Proc Natl Acad Sci USA* 114, E6830–E6838.
- Montgomery A, Garbouchian A, Bentley M (2022). Visualizing vesicle-bound kinesins in cultured hippocampal neurons. *Methods Mol Biol* 2431, 239–247.
- Morin PJ, Sparks AB, Korinek V, Barker N, Clevers H, Vogelstein B, Kinzler KW (1997). Activation of beta-catenin-Tcf signaling in colon cancer by mutations in beta-catenin or APC. *Science* 275, 1787–1790.
- Muresan V, Abramson T, Lyass A, Winter D, Porro E, Hong F, Chamberlin NL, Schnapp BJ (1998). KIF3C and KIF3A form a novel neuronal heteromeric kinesin that associates with membrane vesicles. *Mol Biol Cell* 9, 637–652.
- Nabb AT, Bentley M (2022). NgCAM and VAMP2 reveal that direct delivery and dendritic degradation maintain axonal polarity. *Mol Biol Cell* 33, ar3.
- Nabb AT, Frank M, Bentley M (2020). Smart motors and cargo steering drive kinesin-mediated selective transport. *Mol Cell Neurosci* 103, 103464.
- Navone F, Consalez GG, Sardella M, Caspani E, Pozzoli O, Frassoni C, Morlacchi E, Sitia R, Sprocati T, Cabibbo A (2001). Expression of KIF3C kinesin during neural development and in vitro neuronal differentiation. *J Neurochem* 77, 741–753.
- Nishimura T, Kato K, Yamaguchi T, Fukata Y, Ohno S, Kaibuchi K (2004). Role of the PAR-3-KIF3 complex in the establishment of neuronal polarity. *Nat Cell Biol* 6, 328–334.
- Niwa S, Tanaka Y, Hirokawa N (2008). KIF1B β - and KIF1A-mediated axonal transport of presynaptic regulator Rab3 occurs in a GTP-dependent manner through DENN/MADD. *Nat Cell Biol* 10, 1269–1279.
- Pan X, Acar S, Scholey JM (2010). Torque generation by one of the motor subunits of heterotrimeric kinesin-2. *Biochem Biophys Res Commun* 401, 53–57.
- Phillips RK, Peter LG, Gilbert SP, Rayment I (2016). Family-specific kinesin structures reveal neck-linker length based on initiation of the coiled-coil. *J Biol Chem* 291, 20372–20386.
- Prevo B, Scholey JM, Peterman EJG (2017). Intraflagellar transport: mechanisms of motor action, cooperation, and cargo delivery. *FEBS J* 284, 2905–2931.
- Ren J, Wang S, Chen H, Wang W, Huo L, Feng W (2018). Coiled-coil 1-mediated fastening of the neck and motor domains for kinesin-3 autoinhibition. *Proc Natl Acad Sci USA* 115, E11933–E11942.
- Robinson MS, Sahlender DA, Foster SD (2010). Rapid inactivation of proteins by rapamycin-induced rerouting to mitochondria. *Dev Cell* 18, 324–331.
- Ruane PT, Gummy LF, Bola B, Anderson B, Wozniak MJ, Hoogenraad CC, Allan VJ (2016). Tumour suppressor adenomatous polyposis coli (APC) localisation is regulated by both kinesin-1 and kinesin-2. *Sci Rep* 6, 1–14.
- Sampo B, Kaech S, Kunz S, Banker G (2003). Two distinct mechanisms target membrane proteins to the axonal surface. *Neuron* 37, 611–624.
- Sardella M, Navone F, Rocchi M, Rubartelli A, Viggiano L, Vignali G, Consalez GG, Sitia R, Cabibbo A (1998). KIF3C, a novel member of the kinesin superfamily: sequence, expression, and mapping to human chromosome 2 at 2p23. *Genomics* 47, 405–408.
- Schnapp BJ (2003). Trafficking of signaling modules by kinesin motors. *J Cell Sci* 116, 2125–2135.
- Scholey JM (2013). Kinesin-2: a family of heterotrimeric and homodimeric motors with diverse intracellular transport functions. *Annu Rev Cell Dev Biol* 29, 443–469.
- Sheetz MP (1987). What are the functions of kinesin? *BioEssays* 7, 165–168.
- Silverman MA, Kaech S, Ramser EM, Lu X, Lasarev MR, Nagalla S, Banker G (2010). Expression of kinesin superfamily genes in cultured hippocampal neurons. *Cytoskeleton* 67, 784–795.
- Soda T, Gen Y, Terasaki K, Iwai N, Kitaichi T, Dohi O, Taketani H, Seko Y, Umemura A, Nishikawa T, et al. (2022). Loss of KAP3 decreases intercellular adhesion and impairs intracellular transport of laminin in signet ring cell carcinoma of the stomach. *Sci Rep* 12, 5050.
- Stetler A, Winograd C, Sayegh J, Cheever A, Patton E, Zhang X, Clarke S, Ceman S (2006). Identification and characterization of the methyl arginines in the fragile X mental retardation protein Fmrp. *Hum Mol Genet* 15, 87–96.
- Takeda S, Yamazaki H, Seog DH, Kanai Y, Terada S, Hirokawa N (2000). Kinesin superfamily protein 3 (KIF3) motor transports fodrin-associating vesicles important for neurite building. *J Cell Biol* 148, 1255–1265.
- Tas RP, Chazeau A, Cloin BMC, Lambers MLA, Hoogenraad CC, Kaptein LC (2017). Differentiation between oppositely oriented microtubules controls polarized neuronal transport. *Neuron* 96, 1264–1271.e5.
- Teng J, Rai T, Tanaka Y, Takei Y, Nakata T, Hirasawa M, Kulkarni AB, Hirokawa N (2005). The KIF3 motor transports N-cadherin and organizes the developing neuroepithelium. *Nat Cell Biol* 7, 474–482.
- Twelvetrees AE (2020). The lifecycle of the neuronal microtubule transport machinery. *Semin Cell Dev Biol* 107, 74–81.
- Twelvetrees AE, Lesept F, Holzbaur ELF, Kittler JT (2019). The adaptor proteins HAP1a and GRIP1 collaborate to activate the kinesin-1 isoform KIF5C. *J Cell Sci* 132, 1–9.
- van Bommel B, Konietzny A, Kobler O, Bär J, Mikhaylova M (2019). F-actin patches associated with glutamatergic synapses control positioning of dendritic lysosomes. *EMBO J* 38, e101183.
- Verhey KJ, Hammond JW (2009). Traffic control: regulation of kinesin motors. *Nat Rev Mol Cell Biol* 10, 765–777.
- Verhey KJ, Kaul N, Soppina V (2011). Kinesin assembly and movement in cells. *Annu Rev Biophys* 40, 267–288.
- Verhey KJ, Lizotte DL, Abramson T, Barenboim L, Schnapp BJ, Rapoport TA (1998). Light chain-dependent regulation of kinesin's interaction with microtubules. *J Cell Biol* 143, 1053–1066.
- Verhey KJ, Meyer D, Deehan R, Blenis J, Schnapp BJ, Rapoport TA, Margolis B (2001). Cargo of kinesin identified as JIP scaffolding proteins and associated signaling molecules. *J Cell Biol* 152, 959–970.
- Wedaman KP, Meyer DW, Rashid DJ, Cole DG, Scholey JM (1996). Sequence and submolecular localization of the 115-kD accessory subunit of the heterotrimeric kinesin-II (KRP85/95) complex. *J Cell Biol* 132, 371–380.
- Weiner AT, Thyagarajan P, Shen Y, Rolls MM (2021). To nucleate or not, that is the question in neurons. *Neurosci Lett* 751, 135806.
- Woll KA, Guzik-Lendrum S, Benseal BM, Bhanu NV, Dailey WP, Garcia BA, Gilbert SP, Eckenhoff RG (2018). An allosteric propofol-binding site in kinesin disrupts kinesin-mediated processive movement on microtubules. *J Biol Chem* 293, 11283–11295.
- Woźniak MJ, Allan VJ (2006). Cargo selection by specific kinesin light chain 1 isoforms. *EMBO J* 25, 5457–5468.
- Xia T, Li N, Fang X (2013). Single-molecule fluorescence imaging in living cells. *Annu Rev Phys Chem* 64, 459–480.
- Yamazaki H, Nakata T, Okada Y, Hirokawa N (1995). KIF3A/B: a heterodimeric kinesin superfamily protein that works as a microtubule plus end-directed motor for membrane organelle transport. *J Cell Biol* 130, 1387–1399.
- Yamazaki H, Nakata T, Okada Y, Hirokawa N (1996). Cloning and characterization of KAP3: a novel kinesin superfamily-associated protein of KIF3A/3B. *Proc Natl Acad Sci USA* 93, 8443–8448.
- Yang R, Bostick Z, Garbouchian A, Luisi J, Banker G, Bentley M (2019). A novel strategy to visualize vesicle-bound kinesins reveals the diversity of kinesin-mediated transport. *Traffic* 20, 851–866.
- Yang Z, Goldstein LSB (1998). Characterization of the KIF3C neural kinesin-like motor from mouse. *Mol Biol Cell* 9, 249–261.
- Yogev S, Shen K (2017). Establishing neuronal polarity with environmental and intrinsic mechanisms. *Neuron* 96, 638–650.